NASA TECHNICAL MEMORANDUM

NASA TM X-62,285

NASA TM X-62,285

FLIGHT TEST RESULTS FROM THE CV990 SIMULATED SPACE SHUTTLE DURING UNPOWERED AUTOMATIC APPROACHES AND LANDINGS

Frederick G. Edwards and John D. Foster

Ames Research Center
Moffett Field, California 94035

August 1973

FLIGHT TEST RESULTS FROM THE CV990 SIMULATED SPACE SHUTTLE DURING UNPOWERED AUTOMATIC APPROACHES AND LANDINGS

Frederick G. Edwards and John D. Foster

Ames Research Center
Moffett Field, California 94035

SUMMARY

Unpowered automatic approaches and landings with a CV990 aircraft were conducted to study navigation, guidance, and control problems associated with terminal area approach and landing for the space shuttle. The flight tests were designed to study from 11,300 m to touchdown the performance of a navigation and guidance concept which utilized blended radio/inertial navigation using VOR, DME, and ILS as the ground navigation aids. In excess of fifty automatic approaches and landings were conducted. Preliminary results indicate that this concept may provide sufficient accuracy to accomplish automatic landing of the shuttle orbiter without air-breathing engines on a conventional size runway.

INTRODUCTION

The Space Shuttle Vehicle must be able to perform landings on a conventional size runway in either an automatic or piloted (manual) mode. Since the shuttle will fly and respond much like a large jet transport aircraft during the approach and landing, a significant transfer of jet transport autoland technology is expected. However, the SSV is in many ways different from a large jet transport. For example, the shuttle will have a lower maximum L/D and will be unpowered in the approach. Based on these differences, it appeared that research was necessary to develop a technology base for the design of the terminal navigation, guidance, and control (GN&C) system for the SSV. This research would establish the navigation system, guidance laws, and the guidance and control equipment and instrumentation necessary to accomplish automatic and manual control from the end of reentry to the ground. To meet the needs of the Space Shuttle Program the Ames Research Center initiated plans early in the program to develop a capability for flight test validation of SSV navigation, guidance, and control concepts. Comprehensive analysis and ground based simulation studies of the shuttle landing approach have been performed by Ames and its contractors (reference 1-4). Some flight tests at FRC (references 5-6) demonstrated the feasibility of unpowered approaches and landings of low L/D vehicles under manual control, however, no flight work had been conducted with a completely automatic guidance, navigation, and control system.

An exaimination of candidate aircraft suitable for the project indicated that NASA's Convair 990 (CV990) had the capability of simulating the orbiter lift-to-drag characteristics over the entire velocity spectrum of interest (i.e., terminal area, final approach, and landing phases of flight). In June 1971, a contract was signed with Sperry Flight Systems Division to provide a digital avionics system for installation in the CV990. The system, referred to as the Simulated Shuttle Flight Test System (SS-FTS), was to have sufficient size, speed, and flexibility to mechanize the unpowered navigation, guidance, and control terminal area concepts postulated for the orbiter. The system installation and checkout in the CV990 was completed on June 1, 1972 and flight tests were initiated on June 2, 1972. A total of 18 flights have been conducted during three flight test periods in June, August, and October-November 1972.

SYMBOLS

AGL	Above Ground Level
ARC	Ames Research Center
CADS	Central Air Data System
CAS	Calibrated Air Speed
DME	Distance Measuring Equipment
EAFB	Edwards Air Force Base (USAF)
FRC	Flight Research Center
GSIP	Glide Slope Intercept Point
G/S	ILS Glide Slope
H, h	Altitude (H = -Z)
IAS	Indicated Air Speed
ILS	Instrument Landing System
INS	Inertial Navigation System
L/D	Aerodynamic Lift to Drag Ratio
LOC	ILS Localizer
RCS	Runway Coordinate System
R_o	R-Zero Circle
S/B	Speed Brakes
SS-FTS	Simulated Shuttle Flight Test System
SSV	Space Shuttle Vehicle
TACAN	Tactical Air Navigation
TOL	Take-Off and Landing Facility
UHF	Ultra-high Frequency
VHF	Very High Frequency
VOR	Very High Frequency Omnirange
X	Longitudinal Coordinate in RCS
Y	Lateral Coordinate in RCS

Z	Vertical Coordinate in RCS (Z = -H)
γ	Flight Path Angle
ℓ	Centerline
ε	Error
σ	Standard Deviation

Subscripts

act	actual
err	error
est	estimate
R	radar
ref	reference
G	guidance
N	navigation

SYSTEM CONCEPTS

The components of the avionics system installed in the CV990 are shown on figure 1. It is an integrated digital avionics system performing all the terminal area navigation, guidance, and control in the CV990 flight test vehicle. It is an adaptation of the G&N system which Boeing had selected for installation in its supersonic transport. This system provides NASA with a flexible research facility for inflight evaluation of terminal area, approach and landing problems of the space shuttle.

The system is capable of performing either automatic or piloted landings. These tests have concentrated on the use of conventional radio/navigation aids which are well understood and widely used. The system was configured as a blended inertial radio navigation system. An indepth discussion of each of the system components, their function and operation is presented in reference 7.

In order to put the flight test data in perspective, a typical trajectory which was flown during these flight tests will be discussed, as well as the navigation concept, the flight conditions, and the operational procedures. Only a limited discussion of these items is presented herein. The reader is referred to references 7 and 8 for more operational details and a complete discussion of the guidance, navigation, and control equations.

The tests were conducted at Edwards Air Force Base with all landings on the 4,570 m main runway (Runway 22).

Conventional CV990 procedures were followed during aircraft takeoff and climb to 11,300 m. Before initiating the transition from conventional transport to the simulated shuttle vehicle it was necessary to input data to the system relative to the chosen landing site, the navigation aids to be used, and the aircraft weight. This was accomplished by the pilot via the Data Entry Panel (Keyboard) and the Status Panel (Display). The computer requested the information via the Status Panel. The pilot entered the appropriate response to the computer display via the Keyboard. Simulated shuttle operation was initiated by tuning the selected radio/navigation aids (i.e., DME, DME/VOR) selecting the SSV switch position, pressing the AUTO Button on the Mode Select Panel, deploying the speed brake and landing gear and retarding the throttles to flight idle. From this point on, the complete approach through touchdown was automatic, with the exception of a final speed brake adjustment and flap deployment during the last stages of the approach.

Figures 2a and 2b show a typical approach trajectory and indicates the guidance and navigation concepts implemented for each of the phases of the approach from 11,300 m to touchdown.

The energy management phase was designed to align the vehicle with the runway heading at the top of the two-segment approach path with sufficient energy to insure an ability to reach the runway. The maneuver is based on a fixed, imaginary vertical cylinder (called the R-Zero circle) which was about eight nautical miles in diameter with its axis on an extension of

the runway centerline. Regardless of the direction of the initial approach, the descending vehicle was first aligned with a tangent to the R-Zero circle in order to transition in a clock-wise path around the circle. The aircraft glided at a near maximum L/D condition (maximum for the simulated shuttle) at about 230 knots (IAS) to the circle and spiraled clock-wise around it until it acquired the outbound raidal which was also tangent to the R-Zero circle. It proceeded outbound along this radial for a distance which was continuously being computed to determine when the aircraft should start the procedure turn inbound to intercept the steep glide slope segment of the two-segment approach path at an altitude above 6,100 m.

Navigation during the energy management phase was performed with the two DME stations (Lake Hughes and George Air Force Base) and the barometric altimeter. The onboard system used these available measurements combined in the computer with the respective inertial velocity components from the INS to give the components of the position estimates.

At approximately 6,100 m , the vehicle intercepted the runway centerline plane, captured the ILS localizer and pitched over to fly the steep glide slope phase. It continued down the steep portion as the velocity increased to a nominal 305 knots (IAS). The rate of descent on the steep glide slope was about 1,830 m per minute, the L/D about five (5).

Navigation during the steep glide slope phase was performed with a single DME station (Lake Hughes), the ILS localizer, and the barometric altimeter.

At about 762 m (AGL), a final speed brake adjustment was annunciated on the Status Panel and made by the pilot. The L/D dropped to approximately 4.5, then gradually increased as the velocity decreased during first flare.

The first flare was initiated at about 420 m (AGL) when the ILS glide slope beam was intercepted. The system captured the ILS glide slope as the aircraft flared to the shallow leg of the approach. The rate of descent was arrested from 1,830 m per minute to about 550 m per minute just after first flare and decreased to about 274 m per minute prior to final flare.

Navigation during the shallow glide slope phase was performed with the ILS localizer and glide slope signals and the barometric altimeter.

At approximately 245 knots on the shallow glide slope, the Status Panel displayed the command to the pilot for flaps equal to 10°. With the airspeed and altitude continuing to decrease, the system was programmed to initiate final flare when the height above the runway was about 18 m. At 2.5 m above the runway, a decrab maneuver was performed to align the aircraft with the centerline of the runway. Touchdown occurred nominally at 175 knots airspeed with about 0.6 m per second rate of descent. The system was disconnected by the pilot at touchdown. Automatic roll-out and braking was not provided.

The approach just described could be flown in an automatic mode or in a manual mode using the side arm controller or the normal aircraft yoke. During manual operation, the pilot centered the flight director needles in order to fly the profile.

Figure 3 shows the CV990 aircraft during the steep glide slope portion of a simulated shuttle approach.

Ground tracking data was obtained from the Flight Research Center MPS19 radar for the high altitude portion of the flight; from a mobile tracking radar located near the touchdown point for the final approach and landing phase; and from the Air Force tracking cinetheodolite stations located along the runway for obtaining precise touchdown data.

RESULTS AND DISCUSSION

The SS-FTS system was functionally tested in both the automatic and the manual flight director mode. Insufficient data was obtained to evaluate the manual mode of operation, thus this report will deal only with the results obtained from the automatic mode of operation. Many automatic approaches and landings were conducted during the course of the test series. An acceptable or optimal set of system gains was not established until part way through the third test period. The data which is presented is from a set of 36 automatic approaches and landings conducted during the latter stages of the third test period, during which time the system gains were invariant.

The performance data is divided into two broad categories (1) guidance performance and (2) navigation performance. Within each category the data is presented at selected positions (windows) along the flight trajectory. The systems performance as measured at these selected positions is presented in the form of Y-Z plots, time histories, histograms, and trajectory plots, etc. A definition of the coordinate system, the "windows", and a definition of the guidance and navigation errors precedes the presentation of the data.

Geometry

Coordinate System - All data presented in this report is referenced to a right-hand Cartesian coordinate system with the origin on the center-line of runway 22 (Edwards Air Force Base), at the ILS Glide Slope intersection point (GSIP). The X-axis is positive along the runway centerline in a southwesterly direction, the Y-axis is positive in a northwesterly direction perpendicular to the X-axis, and Z-axis is positive downward and perpendicular to the X and Y axis. The X and Y-axes are in a plane tangent to the earth at the origin. This coordinate system is known as the Runway Coordinate System (RCS). A graphical description of the RCS is presented in figure 4.

Windows - The location of the three windows for which system performance data will be presented is shown in figure 4. These windows, which are located on an extention of the runway centerline (X-axis) are; (1) the steep glide slope capture window located at X = - 39,200 m (H ≈ 6,100 m); (2) the first flare window located at X = -7,160 m (h ≈ 457 m), and (3) the final flare window located at X = - 487 m (h ≈ 21.4 m).

Definition of the Guidance and Navigation Error - The terms "navigation error" and "guidance error" will be used repeatedly in the discussion of system performance. These terms will be defined with the aid of the graphical representation shown in figure 5. The figure shows a ground plane projection of the "actual" reference trajectory which is geometrically referenced to the RCS origin (GSIP) and the "estimated" reference trajectory which is computed by the onboard system. The disagreement between the "estimated" and "actual" reference trajectory is due to measurement errors (bias and random noise) in the radio/inertial navigation system.

The actual position of the aircraft at any time was determined by ground-base tracking radar and differed from the position estimated by the onboard system by the magnitude of the navigation error. In other words, the navigation error is defined as the time correlated difference between the radar measurement of aircraft position, and the onboard estimate of position. Analyticaly, this error is expressed as:

$$\varepsilon_N = (\tilde{X}_R - \tilde{X}_{est}) + (\tilde{Y}_R - \tilde{Y}_{est}) + (\tilde{H}_R - \tilde{H}_{est})$$

The guidance error was determined solely from data computed onboard the aircraft. An estimate was made for both the position of the aircraft and the position of the reference trajectory. The guidance error is defined as the time correlated difference between these two estimates. Analyticaly, this error is expressed as:

$$\varepsilon_G = (\tilde{X}_{est} - \tilde{X}_{ref}) + (\tilde{Y}_{est} - \tilde{Y}_{ref}) + (\tilde{H}_{est} - \tilde{H}_{ref})$$

The onboard system controlled the aircraft to reduce the guidance error but could not act upon the navigation error since the system was unaware of its existance.

Guidance Performance

For the 36 automatic approaches and landings of the CV990 simulated shuttle vehicle (reported herein) eight of the runs were initiated from approximately 11,300 m altitude, the remaining 28 runs from 7,620 m.

Those trajectories starting at the lower altitude, omit the so-called energy management portion and intiate the approach in a direction inbound to the runway (straight-in-approach).

Energy Management Phase - Runs initiated from 11,300 m may start at different positions within the "cardioid shaped" energy window. Two examples of these runs are designated as flight patterns E and H for convenient reference and are shown pictorially in figures 6a and 6b.

Presented in the top half of each figure is the down-range - cross-range (X versus Y) plot of aircraft position and in the lower part of the figure, the corresponding altitude-down-range (H versus X) plot. Each figure shows two paths; the segmented line represents the reference path or nominal trajectory of the aircraft as computed by the onboard guidance program and the continuous line represents the position of the aircraft as estimated by the onboard system. As previously noted, the time correlated difference between these two paths is the guidance error of the system.

Pattern E - Figure 6a shows the approach profile for a Pattern E. The approach was initialized south of the runway centerline, well within the energy window with the aircraft heading north and closing on the R-Zero circle. The aircraft acquired the R-Zero circle just prior to crossing the extension of the runway centerline, banked right and tracked the R-Zero circle. About 50 seconds later, the aircraft acquired the outbound radial and tracked outbound for about 15 seconds. The final or procedure turn was initiated when the predicted altitude loss during the turn would result in interception of the steep glide slope at approximately 6,100 m. The control system initally commanded a 35° bank angle, but this bank command rapidly increased to the bank angle limit of 45° as the ground speed increased during the turn due to the 40 knot cross-wind. The bank angle constraint restricted the aircraft from following the reference path. The aircraft drifted to the left of the path but recovered during the latter part of the turn as the aircraft headed into the wind. The turn was completed at about 7,020 m altitude with the steep glide slope acquired slightly above 6,100 m.

During the initial run-in to the R-Zero circle the guidance error was quite small. As previously noted, during the final turn maneuver the guidance error became more pronounced as the aircraft was consistently drifting to the left of the reference path. The maximum guidance error during the approach occurred about half way through the final turn and was 1,585 m.

Pattern H - Figure 6b illustrates a trajectory in which the system was effectively initialized outside the energy window even though this fact was not immediately apparent. The approach was initialized north of the runway centerline and appeared to be within the energy window but quite close to the boundry. The onboard estimate of the aircraft position was displaced from the actual initiation point (from radar) by about 1-1/2 nautical miles. This discrepency, due to the INS drifts, is not significant as long as the aircraft is still within the window. However, in this case the aircraft was off in heading by 30° to the right and low on initial velocity (M = .80), which placed it, in essence, outside the energy window. After the navigation system was updated via the radio navigation aids (DME-DME), the aircraft corrected the position estimate and heading error, started closing the range to the R-Zero circle and acquired the circle about half a minute later. The R-Zero circle was tracked for about 2-1/2 minutes with the aircraft flying close to maximum L/D, descending at 1,220 m /minute. At the intercept of the outbound radial a low altitude (energy) condition existed. The system therefore omitted the outbound radial phase; immediately proceeded into the final turn, and attempted to make a minimum radius turn. During the turn the aircraft dirfted left of the desired path due to the winds and the limited bank angle authority. For the entire approach, the aircraft altitude was lower than desired and at completion of the final turn the aircraft was 1,500 feet below the steep glide slope. Flying at maximum L/D, the aircraft finally intercepted and captured the steep glide slope at an altitude of 5,340 m. This indicates that the initial condition constraints were violated since capture should nominally occur above 6,100 m.

Guidance Error at Steep Glide Slope Capture Window - The guidance errors at the steep glide slope window (X = -39,200 m , h ≈ 6,100 m) for all of the high altitude runs are shown in figure 7. At this window location, the guidance error is zero if the aircraft is on the computed runway centerline and on the computed steep glide slope beam at 6,100 m above ground level. The four runs which show large negative vertical errors in figure 7 are those in which the aircraft began with low energy and had not captured the steep glide slope at or above 6,100 m. In these runs, identified by a vertical dash above the data point, the pitch guidance was still in the high altitude energy management mode. Consequently, the system did not try to zero the guidance error directly but rather held the aircraft to a near maximum L/D until it penetrated the steep glide slope at an altitude below 6,100 m . The remaining runs shown in figure 7 are those where capture of the steep glide slope occurred at or above 6,100 m. In these cases, the pitch guidance is in the steep glide slope tracking mode and as a result, the vertical guidance errors are relatively small.

The large lateral errors shown in the figure (i.e., flight 3 circle symbol) results from the limited bank angle authority with the accompaning inability to correct for the effects of high altitude winds.

The data point corresponding to patterns E and H (discussed in the previous section) are designated as flight 7 and 5 respectively in this figure.

Steep Glide Slope Tracking - Shown in figure 8 is a time history of the tracking performance of the system during the steep glide slope phase of the approach. The envelopes of maximum vehicle excursions for the series of automatic approaches are shown as the shaded regions in the figure. The vertical tracking error relative to the 10° glide slope is shown in the upper part of the figure. The lateral tracking error relative to the center of the ILS localizer signal is shown in the lower part of the figure.

A solid trace within the shaded region is a time history of vertical and lateral guidance errors for one specific run which is considered to be an example of "good tracking performance". It is significant to note that at steep glide slope capture, the lateral guidance errors may be larger than 91.5 m but that these errors converged to relatively small values (<24 m) prior to first flare.

Guidance Error at First Flare Window - Figure 9 illustrates the guidance error measured at the first flare window (X = -7,160 m , H ≈ 457 m). The reference in this case is the center of the ILS localizer signal and the center of the steep glide slope as computed by the navigation equations using a single DME and the baro-altimeter. If the guidance errors were zero, the data points would be clustered on the estimated glide slope centerline which is the origin of the graph.

For these data, the vertical mean error is zero with the lateral mean error 3.1 m to the left. The one-sigma error about the mean is ±6.1 m in the vertical direction and ±9.2 m in the lateral direction.

First Flare Altitude - The altitude at which the first flare occurred is presented in figure 10. The data is presented in the form of a histogram; that is, the height of the vertical bar indicates the number of times the aircraft initiated the flare maneuver within a given altitude zone. Each altitude zone is 6.1 m in height. Nominally the aircraft would initiate first flare at a point .97° above the center of the 2.5° glide slope beam. This corresponded to an altitude of 426 m above the ground. The data indicated that the mean flare initiation altitude was 441 m above the ground (a bias of +14.3 m) with a one-sigma dispersion of ±10.4 m These errors could be attributed to either the ILS ground transmitter or the airborne receiver. In terms of the ground transmitted ILS glide slope beam parameters, the errors correspond to a beam bias of +.08° (i.e., beam angle = 2.58° rather than 2.50°) and a random error of ±.05°. From a separate analysis of the Edwards Air Force Base ILS beam characteristic (unpublished) it was found that the day to day variation of the glide slope beam elevation angle could be as large as ±0.2°.

Another possible source of error was from the airborne glide slope receiver. In terms of the parameters for the receiver, the errors (H_{bias} and σ_H) correspond to a six millivolt bais and ±4 millivolt random noise. These receiver errors are well in excess of the manufacturers performance specification for this equipment. Thus it is tentatively concluded that the inaccuracies in flare initiation altitude were most probably due to vairation in the transmitted ILS beam rather than problems with the receivers. Further investigation of this problem is planned.

Speed Control - Figure 11 shows examples of the speed variation during the appraoch from 11,300 m to touchdown. The aircraft velocity was not controlled directly but tended to converge to a constant calibrated airspeed depending upon the flight path angle (or L/D). From initiation of the approach until steep glide slope capture the aircraft was controlled to fly in the operational L/D mode (energy management). The L/D was essentially constant at the value slightly less than the maximum L/D for the shuttle. The aircraft pitch attitude was controlled to maintain this L/D. During the descent the velocity remains constant at about 230 knots (CAS) until steep glide slope capture. Figure 11 shows this effect for the three approaches with the exception that the velocity for pattern H decayed by about 20 knots just prior to steep glide slope capture. It will be remembered that pattern H was the low energy approach discussed previously (figure 6b). The decrease in velocity occurred as the system pitched the aircraft up to the maximum L/D (maximum for the simulated shuttle) to decrease the rate of descent and stretch the path length.

At steep glide slope capture the simulated shuttle pitched over to fly a -10° glide path. The velocities for each trajectory should converge toward 305 knots.

As previously noted, the speed brakes are deployed at the beginning of the run to yield a desired L/D. The speed brake setting was different for each approach and was chosen to compensate for changes in the aircraft weight. The compensation was rather coarse with incremental 5° changes in

speed brake for each 9,060 kilogram change in aircraft weight. A 5° error in the speed brake setting can result in an error as large as 15 knots (CAS) in the equilibrium velocity.

This speed brake law gives acceptable results. However, a refined speed brake deployment technique based on stored nominal velocity profile and modulated speed brakes could converge all velocities at first flare and landing to within a very narrow dispersion, but this must await additional refinements to the system software and vehicle hardware.

Using the simple speed law presently implemented, the velocity dispersions (1σ) at first flare were about 10 knots. This is shown in figure 12.

The velocity dispersion data at first flare are in the form of a histogram of velocities versus number of occurrances. The figure shows that the mean velocity for 36 approaches was 290 knots (CAS) with a one-sigma dispersion of $\pm$10 knots.

The final speed brake adjustment (see figure 11) was made just prior to first flare ($\approx$ 760 m) in order to compensate for atmospheric winds and error in setting the configuration L/D. This setting was a function of the existing atmospheric winds as measured by the onboard INS. No further speed brake adjustments were made during the remainder of the approach to touchdown. Velocity dispersions at final flare and landing are presented later.

Shallow Glide Slope Tracking - The guidance system performance during the first flare and shallow glide slope modes is shown in both the vertical and horizontal plane in figure 13. The three flight paths are from three landing approaches two of which represent the maximum excursions about the ILS glide slope beam while the third represents a more nominal path. The dispersions are caused primarily by the variation in first flare initiation altitude. As previously noted, the flare mode was engaged when the aircraft descended to a point that was 0.97° above the ILS glide slope. Since the ILS receiver signal was used directly to measure this displacement, the flare initiation altitude varied as a function of the noise on the signal. Variation of $\pm$0.2° were detected in the glide slope beam deflection. The first flare began at about 46.3 m above the ground for the upper path in figure 13, at about 43.1 m above the ground for the middle path, and at about 41.5 m above the ground for the lower path.

The variation in the first flare mode performance affected only the initial tracking performance of the shallow glide slope mode. The vertical errors from the ILS glide slope beam after shallow glide slope mode engagement were reduced to less than 7.6 m at an altitude of 122 m. Tracking errors below this altitude were quite small.

In the horizontal plane, the runway centerline tracking mode was a continuation of the same guidance mode used during the steep glide slope made. During this mode, the lateral guidance error decreased as the aircraft approached the runway. This reduction is also apparent in comparing

the lateral guidance error at the first flare and final flare windows, figures 18 and 23, where the standard deviation of the error reduced from 9.15 m to 3.96 m The primary cause for this effect was the error in the lateral position estimate. The noise in the lateral position estimate was proportional to the product of the localizer beam angular noise and the aircraft distance from the localizer antenna. If the noise on the angular beam had a constant amplitude, then the lateral position estimate error would decrease as the aircraft approached the runway. The ratio of the distance from the aircraft to the localizer antenna at the final flare window to that of the first flare window is 0.44 and the ratio of the lateral error standard deviation at the final flare window to that at the first flare window is 0.37. Hence, the change in distance accounts for a substantial part of the lateral guidance error reduction. Thus, the resulting lateral error is consistant with the idea of a constant noise on the localizer beam.

Guidance Errors at Final Flare Window - Figure 14 shows the system guidance performance at the final flare window. The nominal path was the center the ILS localizer beam and the ILS glide slope beam at a distance of 487 m down-range from the touchdown point. The nominal aircraft altitude was 21.4 m AGL.

A mean of the vertical error shown in the figure is 2.1 m above the glide slope centerline. The standard deviation of the vertical error is ±2.5 m. One probable reason for the aircraft to be consistently above the glide slope could be the effect of the close proximity of the ground plane (i.e., ground effect) which tends to increase the effective lift, arrest the sink rate, and drive the aircraft above the glide slope. This tendency to float above the glide slope prior to final flare was observed in the tracking data and is verified by the guidance errors presented in figure 14. A more precise model of the aircraft ground effect could provide information for optimizing the system gains and improving the performance in this region. The CV990 entered the ground effect at about 37 m above the ground. The effect (on lift) increased in an exponential manner as the aircraft approached the ground.

The mean of the lateral guidance error was zero, which means that on the average the aircraft was tracking the center of the ILS localizer beam. The standard deviation was ± 3.5 m

Final Flare Initiation - Flare initiation should occur when the altitude above the ground equals 9.2 m plus twice the altitude rate (i.e., $H = 9.2 + 2\dot{H}$). Figure 15 maps the final flare points in the H versus $\dot{H}$ phase plane. Nominally the aircraft would be descending at about 4.5 m per second at final flare initiation at 18.3 m altitude. The mean altitude and altitude rate from these data is 17.1 m and 19.1 m per second respectively. The standard deviation of the data is shown in the form of a 1σ dispersion ellipse. This is represented by the shaded area in the figure.

Position Dispersions at Touchdown - Figure 16 presents the position dispersions of the aircraft at touchdown. The data are presented as histograms; with the height of a given vertical bar indicating the number of times the aircraft touched down in a given zone on the runway. Distance along the centerline of the runway is divided into zones at each 64.7 m interval. For example, the aircraft touched down seven times in the zone which lay between the 25.2 m and 305 m position along the runway. The zero position is the glide slope intercept point (GSIP) on the runway. These data are from 36 automatic landings. The mean touchdown point was 305 m beyond the glide slope intercept point with a three-sigma dispersion of 457 m ; or in other words, approximately 99% of the landings were contained within a zone 457 m in length. For comparison with these flight data, the FAA Category II three-sigma criteria for distribution of touchdown for commercial transports is shown as the shaded zone. As can be seen, the touchdowns were well within the limits which have been spelled out in FAA advisory circular No. 20-57A (reference 9), for certification of automatic landing systems on conventional jet transports, wherein they specify a three-sigma value of 685 m.

Across the runway dispersions, or lateral dispersions, are depicted in the figure on the right. The data again is presented as a histogram. The runway centerline is taken as zero. Zones across runway are defined at 1.5 m intervals. The three-sigma dispersion was +11.9 m compared with the FAA criteria of +13.7 m. This lateral dispersion data needs some qualification in that the centerline of the ILS localizer beam at Edwards was biased to the right side of the runway centerline. The localizer offset has been removed from the lateral dispersion data to give a more realistic picture of the system performance with a true Category II ILS. The magnitude of the ILS bias will be evident in the data to be presented showing navigation errors at the first flare and final flare windows.

Speed Dispersion at Touchdown - The histograms of vertical speed calibrated or indicated airspeed, and ground speed at touchdown are shown in figure 17. Plotted is the magnitude of the parameter versus the number of occurrances.

The design vertical speed at touchdown was 0.6 m per second. A mean vertical speed of 0.5 m per second was obtained during the flight tests. This difference is not considered significant.

The system was designed to achieve a calibrated airspeed (CAS) at touchdown of 175 +25 knots. The guidance system has indirect (open loop) control of the CAS through an adjustment of the speed brake at first flare. From the flight test, the data shows a mean of 166 knots and a range of +24 knots (σ = +9 knots). As would be expected, the ground speed at touchdown exhibited a larger dispersion since it was not controlled and was dependent on the local wind conditions. The data shows this larger dispersion with σ = +16 knots. The mean value for the ground speed was 175 knots. Even though the touchdown groundspeeds were as high as 210 knots, no piloting problems were encountered.

The ground winds during these flights varied from a low of zero to a high during one approach of 30 knots, but characteristically the winds were low (> 10 knots).

Navigation Performance

The onboard navigation system uses the available measurement from radio-navigation aids (DME, VOR, ILS) and from onboard measurements (INS, Baro., and radio altimeter) to provide an estimate of the present aircraft position and velocity. Ground based measurements (MPS19 tracking radar) of the aircraft position and velocity were made directly for system performance evaluation. Choosing the radar measurements to be the standard (indicating the actual aircraft position) then the onboard measurement may be compared with it to determine the performance of the onboard system. Navigation system performance data is presented and discussed for each of the three navigation windows (steep glide slope capture, first flare, and final flare). In addition, a trajectory plot and corresponding time histories of navigation errors are presented for one example of a high altitude approach from 11,300 m to touchdown.

Energy Management Phase - The trajectory of the aircraft during the energy management phase and continuing until touchdown is presented in figure 18a. The top half of the figure shows the plot of down-range - cross-range position of the aircraft as estimated by the onboard system and as measured by the ground base tracking radar. The lower half of the figure presents the corresponding altitude down-range plot. The time correlated difference between the two trajectories is the navigation error of the onboard system. The time histories of these navigation errors are presented in figure 18b.

The navigation system was initialized on INS only. At this time, (figure 18a), the estimated aircraft position was at the point indicated by a circle. The ground radar shows that the aircraft was actually about 1-1/2 miles to the west of this point. As the radio navaid information (DME-DME) was introduced, the system updated the position estimate. The onboard position estimate improved over the next 20 seconds until it agreed quite closely with the position as determined by the radar. As the aircraft proceeded on the approach, it is noted that the estimated trajectory was displaced slightly to the northwest of the radar measured trajectory. This displacement could result from a bias in the slant range measurement to the DME stations, an error in the designated location of these stations, or a bias in the DME transmitter/receiver. With the data available it was not possible to isolate the source of the error.

The altitude range plot also shows a discrepency between the radar measured altitude and the onboard estimate of altitude. It was suspected that this discrepency was due to errors in the baro-altimeter. Weather balloon data collected for the day of this flight showed the barometric altitude correction to be about 305 m ; for the altitude range between

9,150 and 12,200 m. The barometric correction below 9,150 m decreases linearily to about 38 m at ground level. The correction correlated directly with the altitude error throughout the approach. This will be shown in the time history plots.

Shown in figure 18b is a time history of the navigation errors from initialization through to touchdown. Presented is the difference between the onboard estimate of position (X_{est}, Y_{est}, H_{est}) and the MPS19 ground radar measurement of position X_R, Y_R, H_R) as a function of time. The times at which significant events occurred are labled for convenient cross reference with the preceding trajectory figure. The total navigation error shown in these traces is a combined effect of errors due to ground navaid/airborne receiver signal bias; off nominal atmosphere effects; possible time skews between airborne and ground data as well as the basic navigation system errors resulting from software/hardware mechanization.

A rather large perturbation in the X error is apparent following first flare. This error occurs as the system switches modes and the onboard position estimate changes from a dependence on DME-LOC-Baro to a dependence on ILS G/S-LOC-Baro. The fact the X_{err} did not go to zero at touchdown is not significant since the computer terminated computation of X estimate when the aircraft over flew the GSIP. This event occurred about five seconds prior to touchdown for the example shown here.

The time history of the Y error shows errors as large as 366 m during the early portion of the approach but these decreased after steep glide slope capture to less than 61 m. At touchdown the Y_{err} appears to be about 61 m. Actually, the aircraft touched down within 4.6 m of the runway centerline as determined by the TOL facility, onboard cameras and the Bell Radar Tracking Data. The onboard navigation estimate agreed with these measurements. The only explanation is that the MPS19 radar data exhibited a bias for this run. For other approaches the radar data did not exhibit biases of this magnitude.

The time history of the altitude error (H_{err}) shows errors as large as 214 m during the initial or high altitude phase of the approach. These are reduced to essentially zero at touchdown. Altitude errors of this magnitude occurred during several of the high altitude approaches and appeared to be attributed to a non-standard atmosphere. For example, during flights on days where the air was warmer than the standard atmosphere, the pressure altimeter read low in comparison with the geometric altitude (from radar track). For the flight shown in figure 18b, a balloon launched radiosond acquired atmospheric data. The dashed line in the figure shows the difference between the pressure altitude and the geometric altitude as determined from the radar tracked radiosond. The altitude error time history correlates closely with radiosond data. The real-time altitude estimate could be improved by measuring the static air temperature and compensating within the navigation filter.

Navigation Error at Steep Glide Slope Capture - Figure 19 shows the navigation error at the steep glide slope window; (X = -39,200 m H ≈ 6,100 m). Here the aircraft normally was on the runway centerline extension. The system was navigating in the DME/DME mode. In this mode the standard deviation of the total position measurement error (vector sum of X_{err}, Y_{err}, and H_{err}) as determined from analysis of the raw DME signals and baro-altimeter signal is 457 m. The navigation system, incorporating inertial blending, reduced this error to a standard deviation of + 94 m for the data shown in this figure. The biases in lateral error of - 97 m were the result of either biases in the onboard navigation receivers or uncertainty in the location of the VOR/DME stations. The VOR/DME locations were obtained from the "IFR-SUPPLEMENT, UNITED STATES EFFECTIVE 9 DEC 1971 TO 1 JAN 1972" which lists such locations to an accuracy of one second of arc (≈ 30 m). The bias in the altitude error was + 47.5 m and can be accounted for predominately as the effect of non-standard atmospheric conditions.

Navigation Error at First Flare Window - Figure 20 shows the difference between the ground measured aircraft position (radar) and the onboard aircraft position estimate as the aircraft passed through a window positioned at the initiation of first flare. The aircraft was nominally at an altitude of 457 m AGL, on the steep glide slope, and on the runway centerline extension, 7,160 m down-range from the RCS origin. The navigation system was in the DME/localizer mode.

The data shows that the aircraft was off to the right of the runway centerline extension for all runs and below the glide slope for all but one run. This consistent offset was due to the fact that the ILS localizer beam bends to the right of the runway. The beam position was measured at the touchdown point on a daily basis during the flight test and its position was found to be to the right of the runway centerline.

Previous analytical studies showed that the standard deviation of the total expected measurement error (one DME range, ILS localizer deviation, baro-altimeter) at this location is 107 m. The standard deviation of the total navigation error from the data presented here is 16.8 m.

It is interesting to note that the data fell into distinct groups. For example, the data group which fell to the far right was collected during a series of runs made on a single day (Flight 6). These data, as well as previous qualitative observation of the ILS beam, show that the ILS localizer beam is not stable. The centerline of the ILS beam drifted significantly from day to day, with the "far right" data group collected on the day when the ILS drift was at its extreme.

Navigation Error at Final Flare Window - The navigation error at final flare is illustrated in figure 21. The aircraft was nominally at an altitude of 21.4 m AGL, on the ILS glide slope beam and on the runway centerline. The navigation system was in the localizer/glide slope mode.

The data in this figure show the previously discussed localizer offset, (i.e., localizer beam is offset to the right). Analytical studies have shown that the standard deviation of the total expected error in the measurement at this location is 12 m. The standard deviation of the total navigation error for the flight data shown here is 5.2 m

CONCLUSIONS

1. Conventional ground navigation aids (DME/VOR, ILS) blended with barometric and inertial data are sufficiently accurate to automatically land the simulated shuttle vehicle with three-sigma touchdown dispersions of ±457 m longitudinally and ±11.9 m laterally. This implies that air breathing engines are not required for automatic landings of the space shuttle vehicle.

2. The DME/DME-Baro-altimeter navigation concept for high altitude energy management had a total position accuracy of ±94 m (1σ) at an altitude of 6,100 m.

3. The low altitude guidance concept converged large vertical and lateral guidance errors at an altitude of 6,100 m to errors with a standard deviation of ±2.5 m vertically and ±3.5 m laterally at an altitude of 21.4 m.

4. No piloting problems were encountered with touchdown ground speeds as high as 210 knots.

5. The CV990 simulated shuttle program has demonstrated the operation, dependability, and inherent flexibility of a programmable digital flight computer for guidance, navigation, and control of the space shuttle in the terminal area approach and landing phases of flight.

REFERENCES

1. Osder, S; Keller, R.: Study of Automatic and Manual Terminal Guidance and Control Systems for Space Shuttle Vehicles, Vol. I. NASA CR 114 400, 1971.

2. Osder, S.; Keller, R.: Study of Automatic and Manual Terminal Guidance and Control Systems for Space Shuttle Vehicles, Vol. II. NASA CR 114 401, 1971.

3. Osder, S; Keller, R.: Study of Automatic and Manual Terminal Guidance and Control Systems for Space Shuttle Vehicles, Final Report Supplement. NASA CR 114 407, 1971.

4. Cockayne, W.; Rusnak, W.: Study of Automatic Flare and Decrab Guidance and Control System for the Space Shuttle Vehicle. NASA CR 114 436, 1971.

5. Kock, Berwin M.; Fuler, Fitzhugh, L.; Drinkwater III, Fred J.: Low L/D Approach and Landing Studies Using a CV990 Aircraft. NASA TN D-6732, 1972.

6. Bray, R. S.; Drinkwater III, Fred J; and White, M. D.: A Fight Study of a Power-Off Landing Technique Applicable to Reentry Vehicles, NASA TN D-323.

7. Hegarty, D. M.: A Functional Description of a Digital Flight Test System for Space Shuttle Navigation and Guidance Research in the Terminal Area. Proposed NASA TMX.

8. Gaylor, Randall: Flight Test System for Study of Space Shuttle Vehicle Guidance and Navigation Concepts. Proposed NASA CR.

9. Advisory Circular NO. 20-57A, Automatic Landing Systems, 12 Jan. 1971, Dept. of Transportation, Fed. Av. Adm.

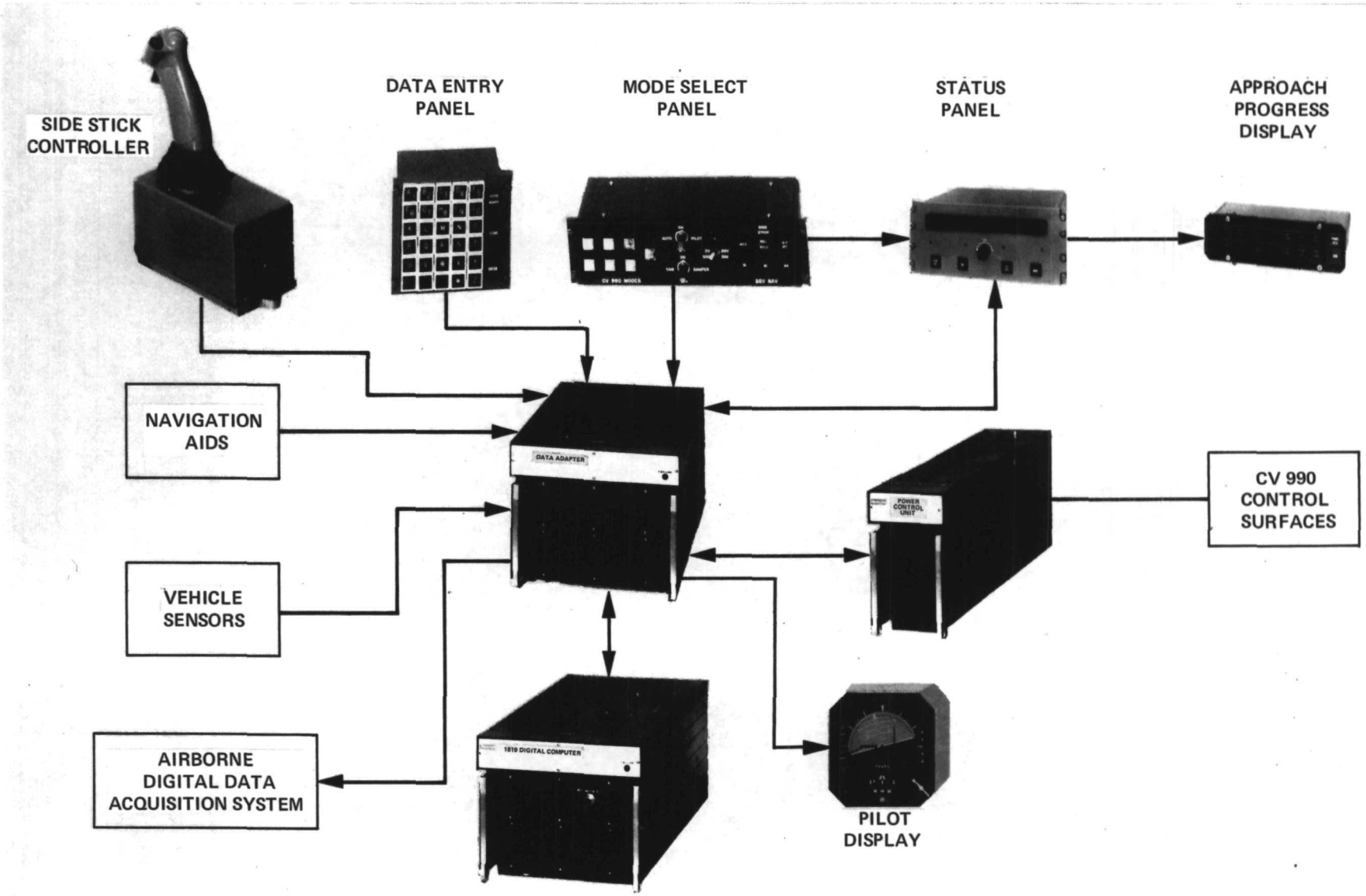

Figure 1. - Block Diagram of the SSV Flight Test System

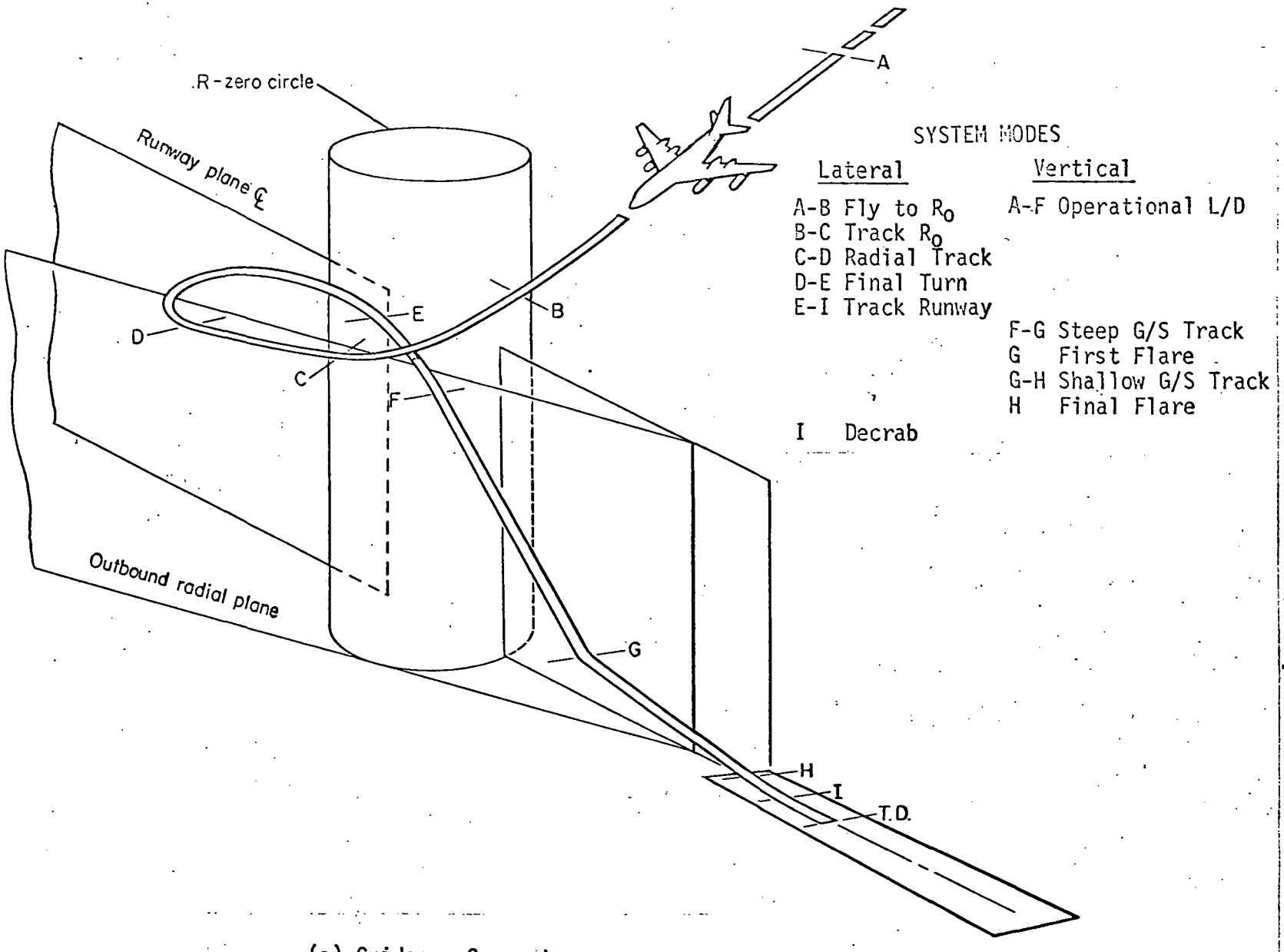

(a) Guidance Concept.

Figure 2. - Approach Trajectory

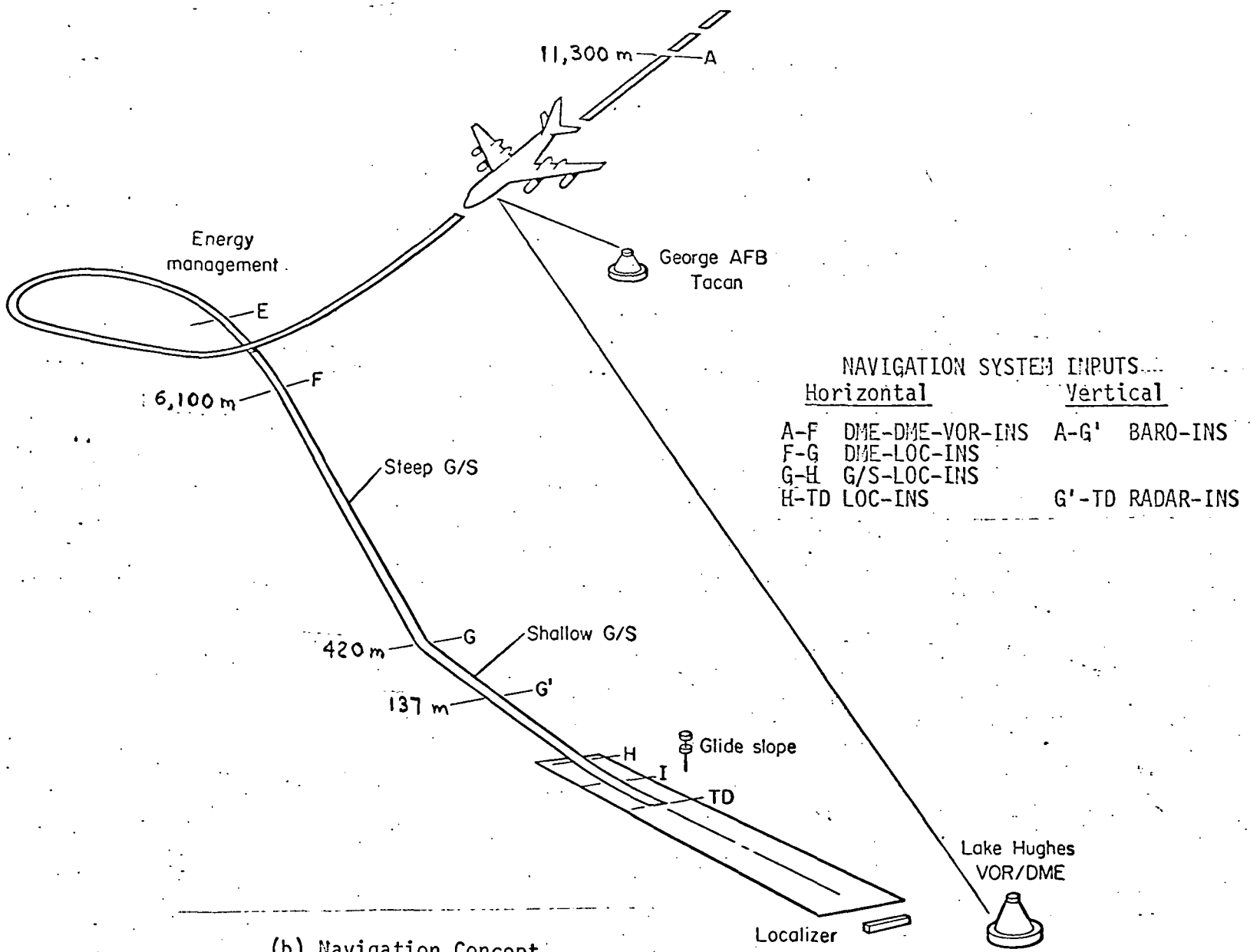

(b) Navigation Concept.

Figure 2. - Concluded

Figure 3. - CV990 Aircraft During Simulated Shuttle Approach

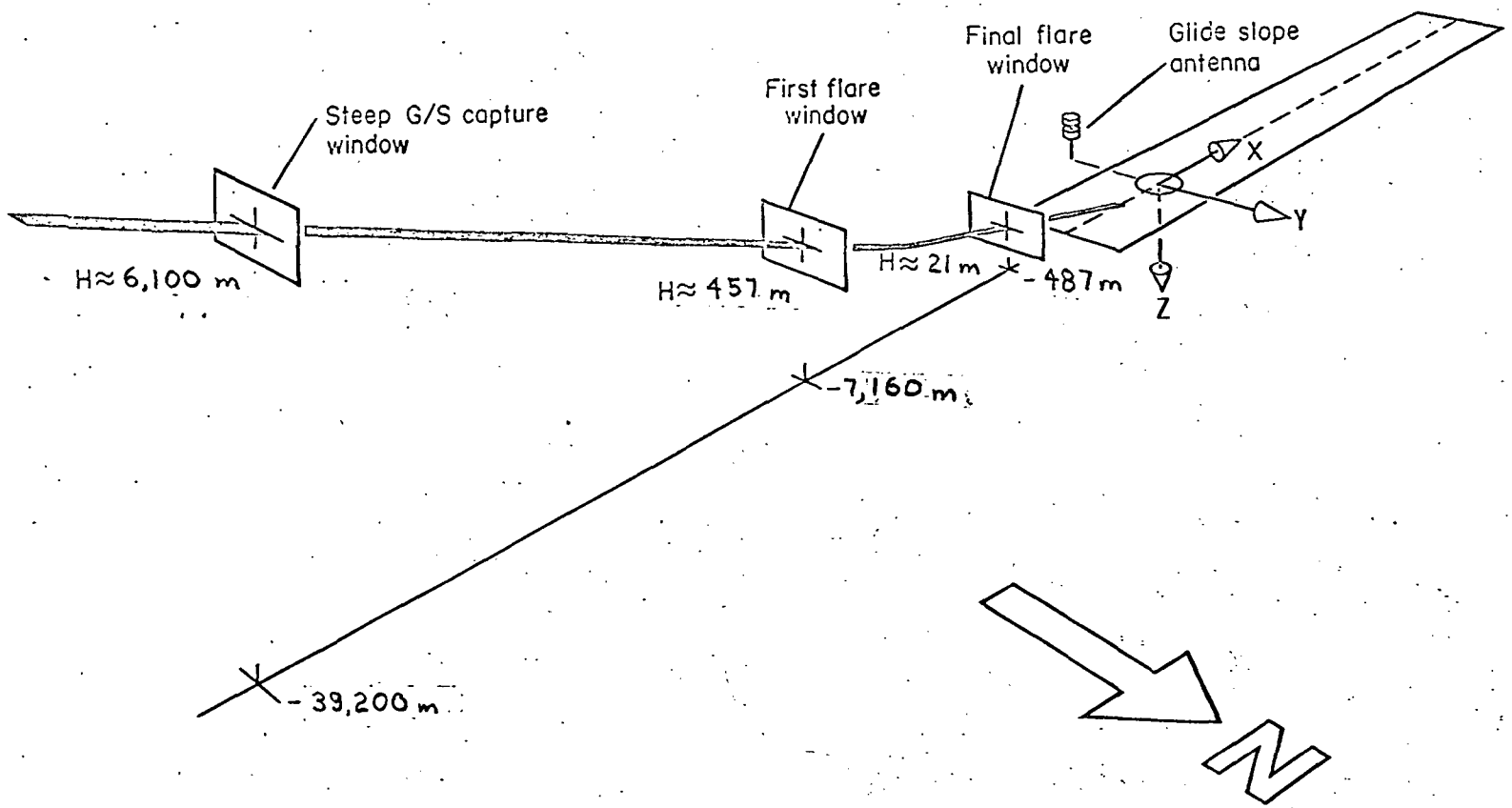

Figure 4. - Guidance and Navigation Window Locations

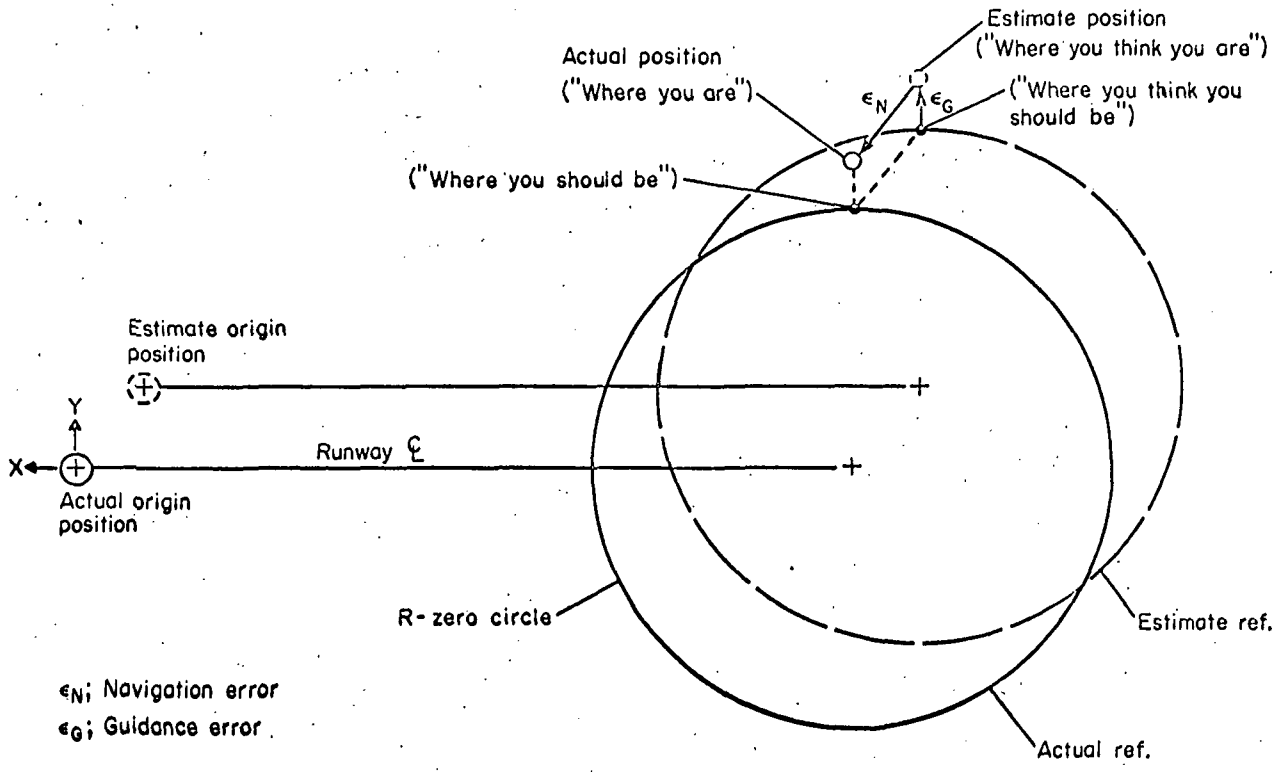

Figure 5. - Graphical Description of Navigation and Guidance Errors

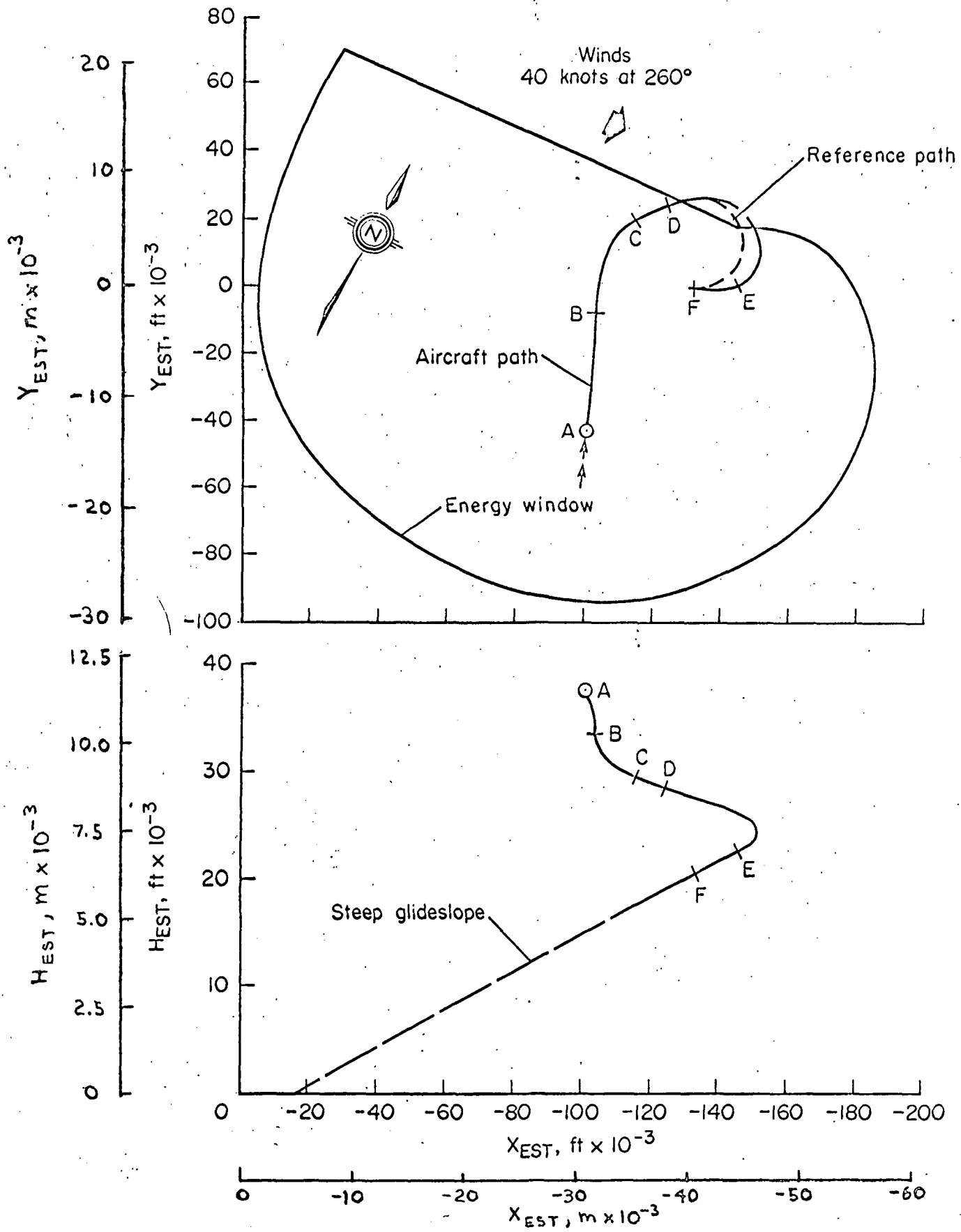

(a) Pattern E.

Figure 6. - Energy Management Phase

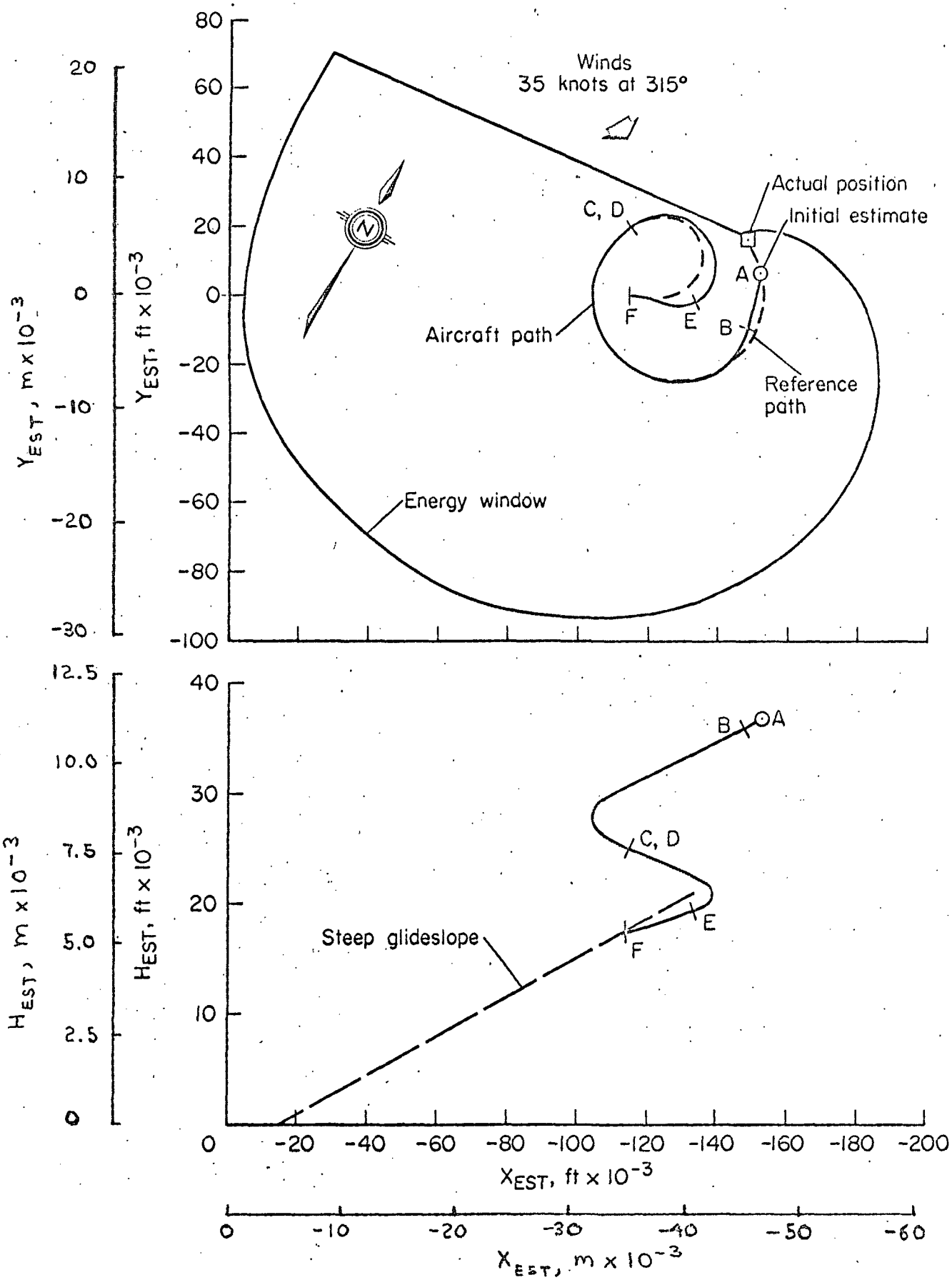

(b) Pattern H

Figure 6. - Concluded

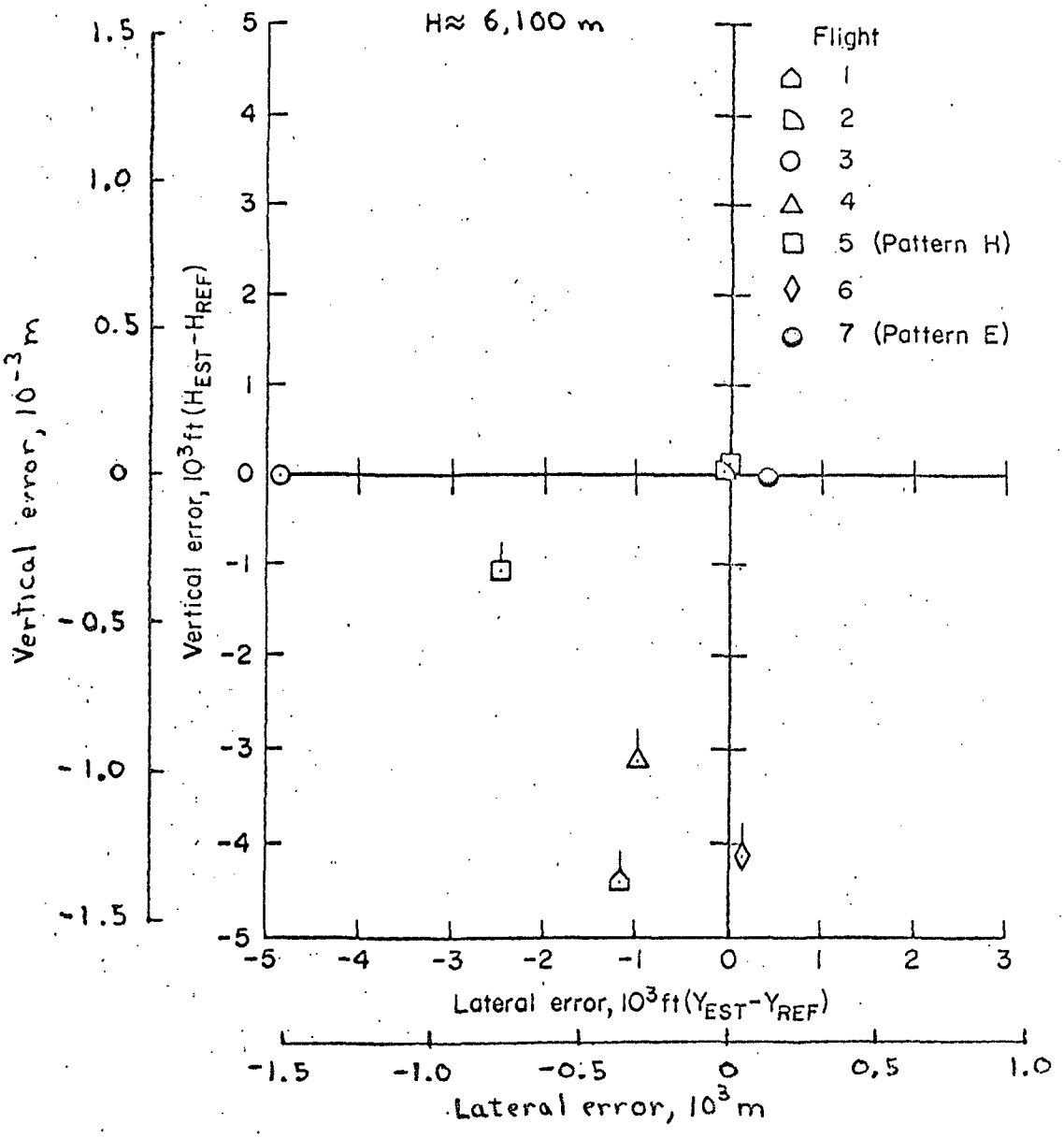

Figure 7. - Guidance Error at Steep Glide Slope Capture Window

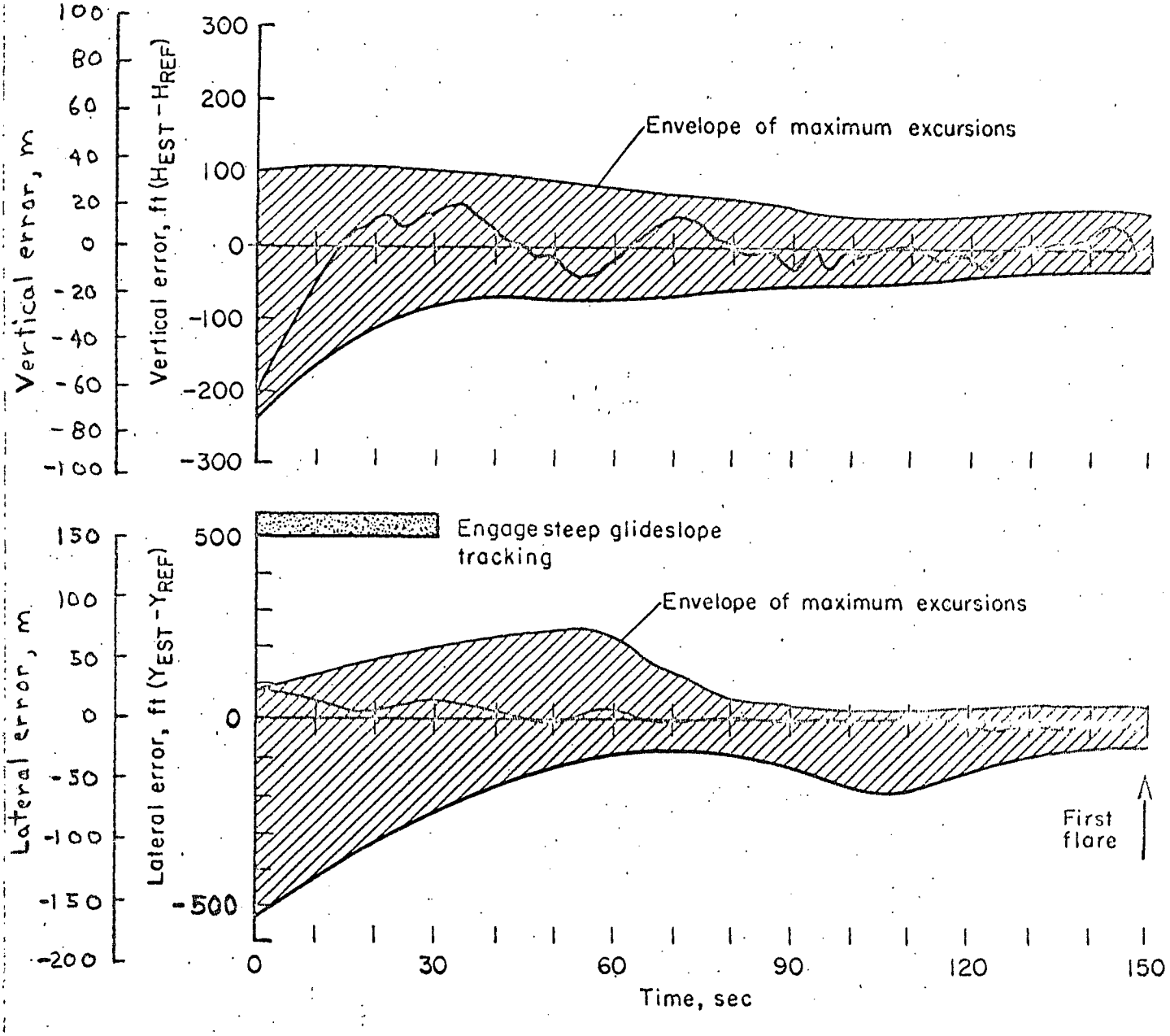

Figure 8.- Steep Glide Slope Tracking

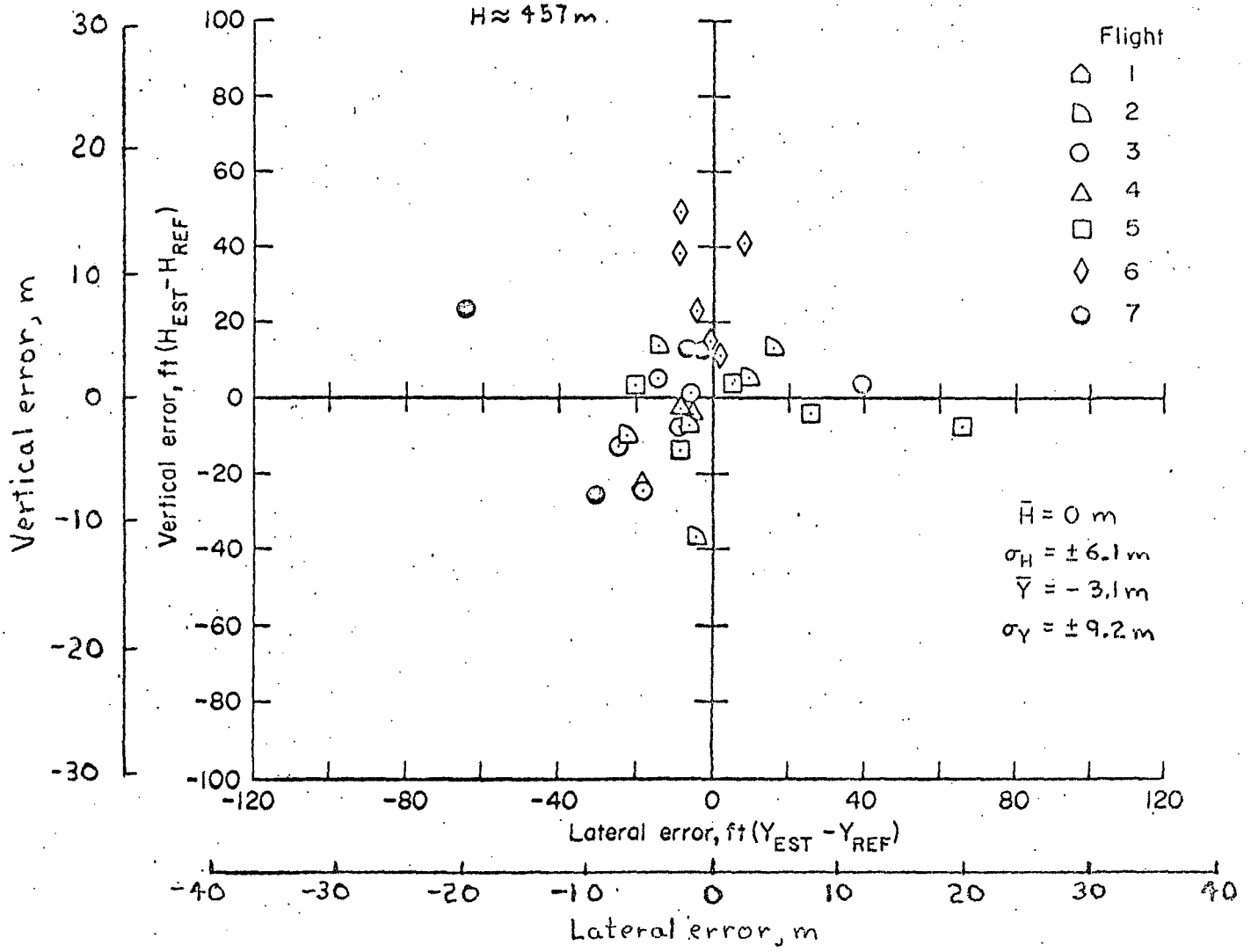

Figure 9. - Guidance Error at First Flare Window

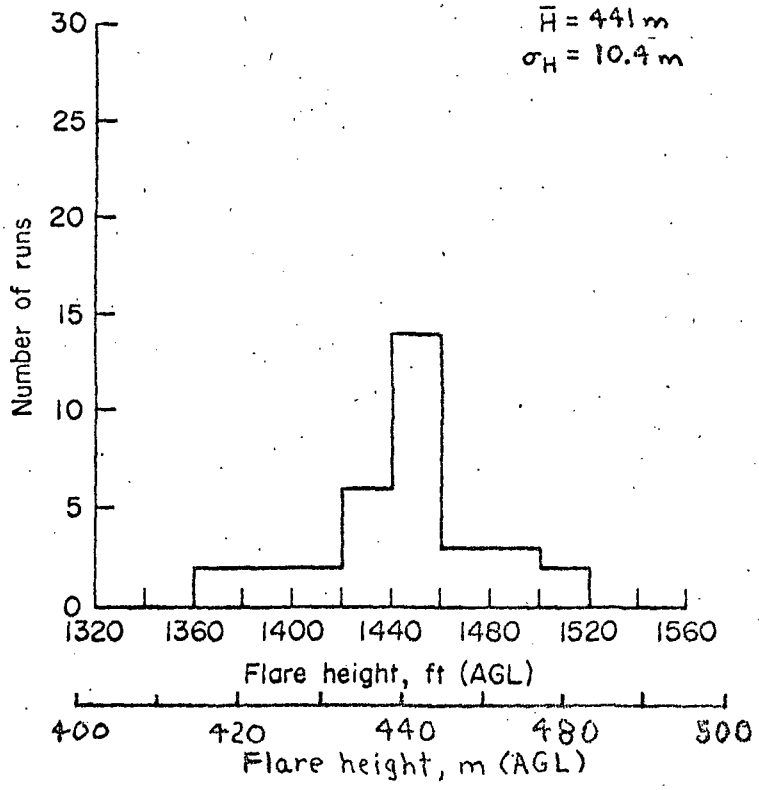

Figure 10. - Altitude of First Flare

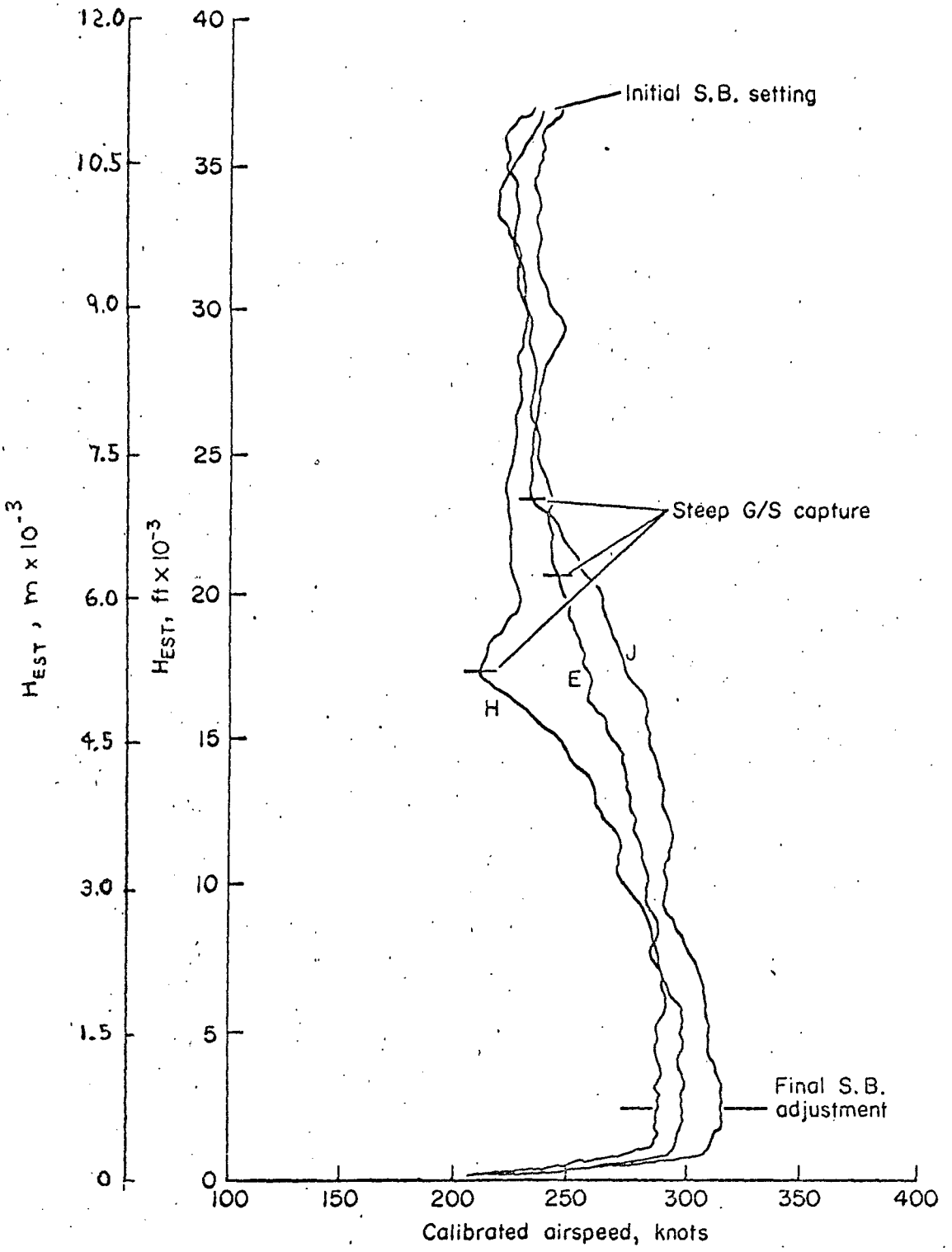

Figure 11. - Speed Control During Approach

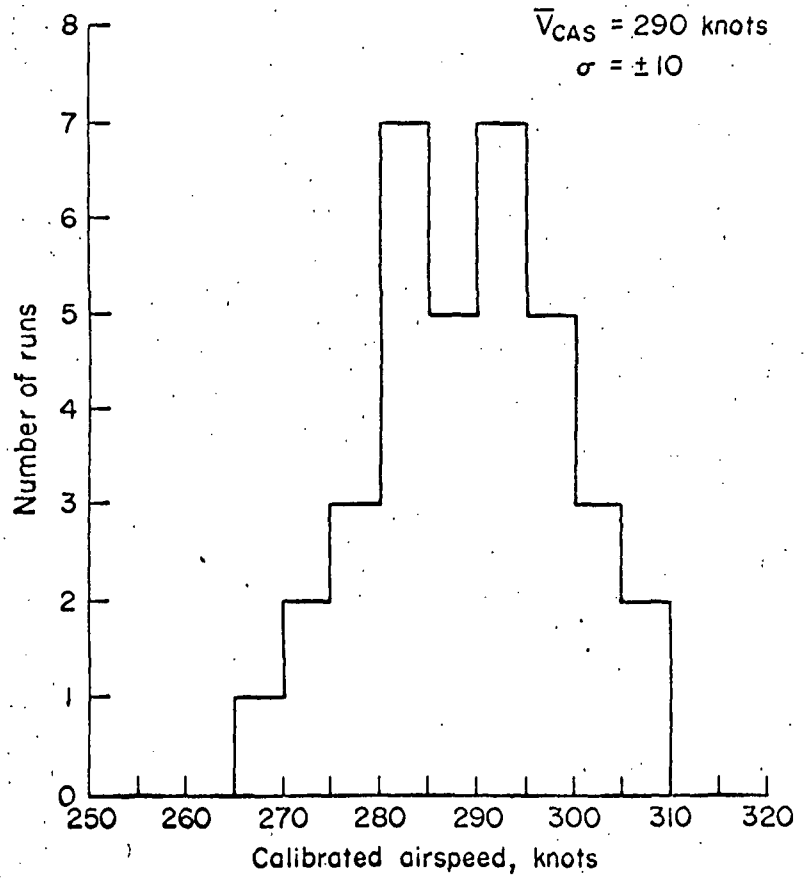

Figure 12. - Airspeed Dispersions at Nominal First Flare Altitude

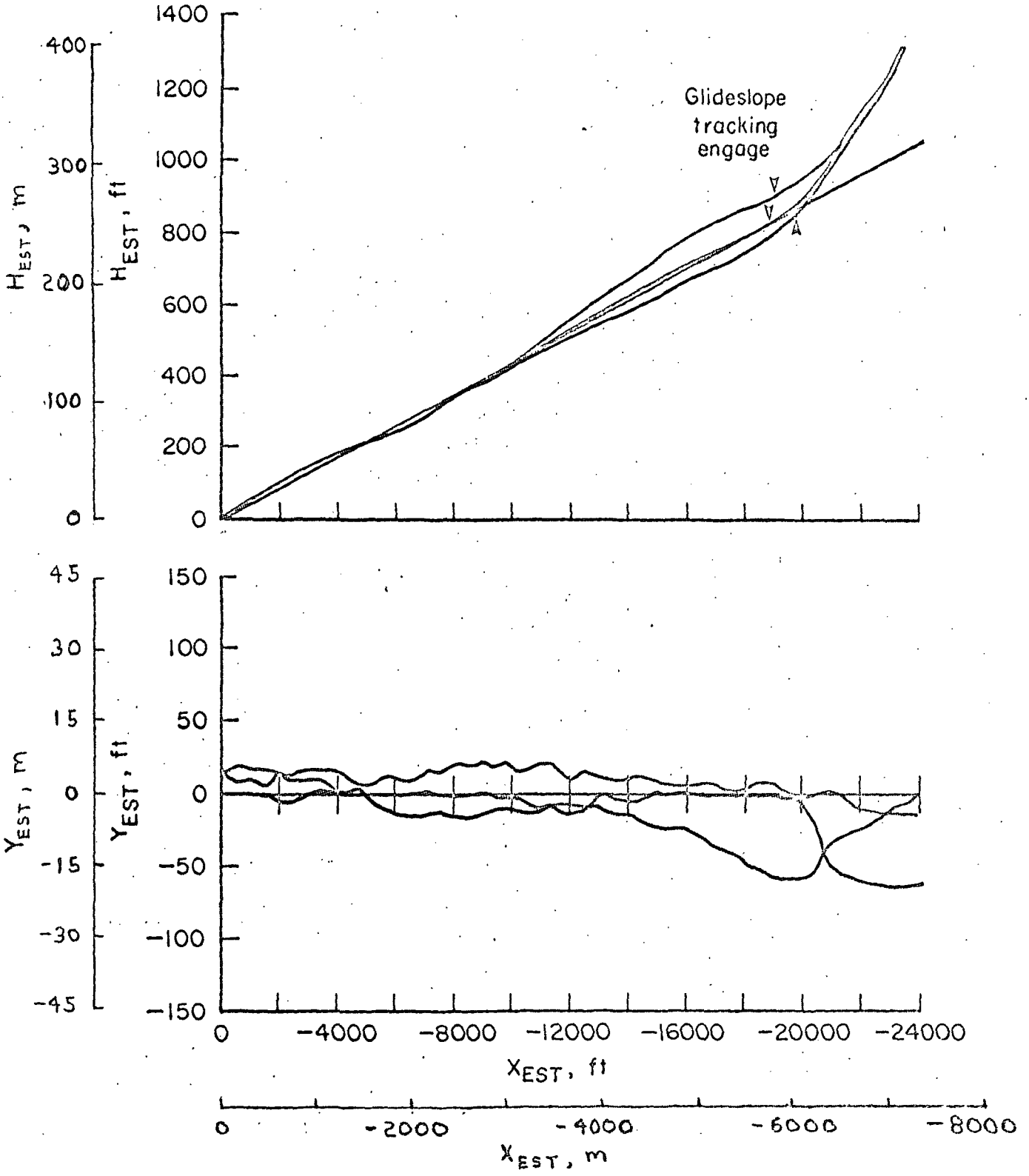

Figure 13. - First Flare and Shallow Glide Slope Tracking Performance

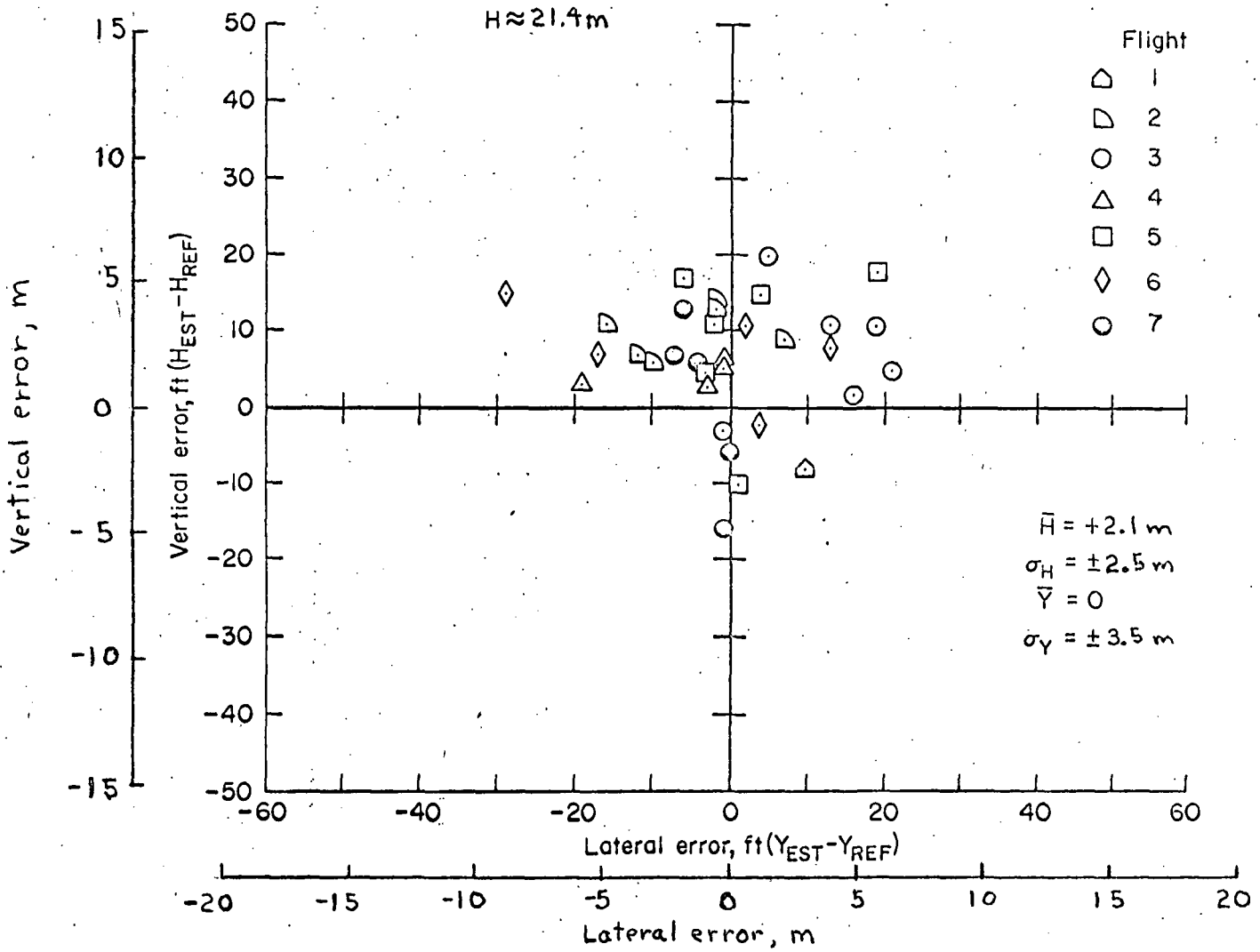

Figure 14. - Guidance Error at Final Flare Window

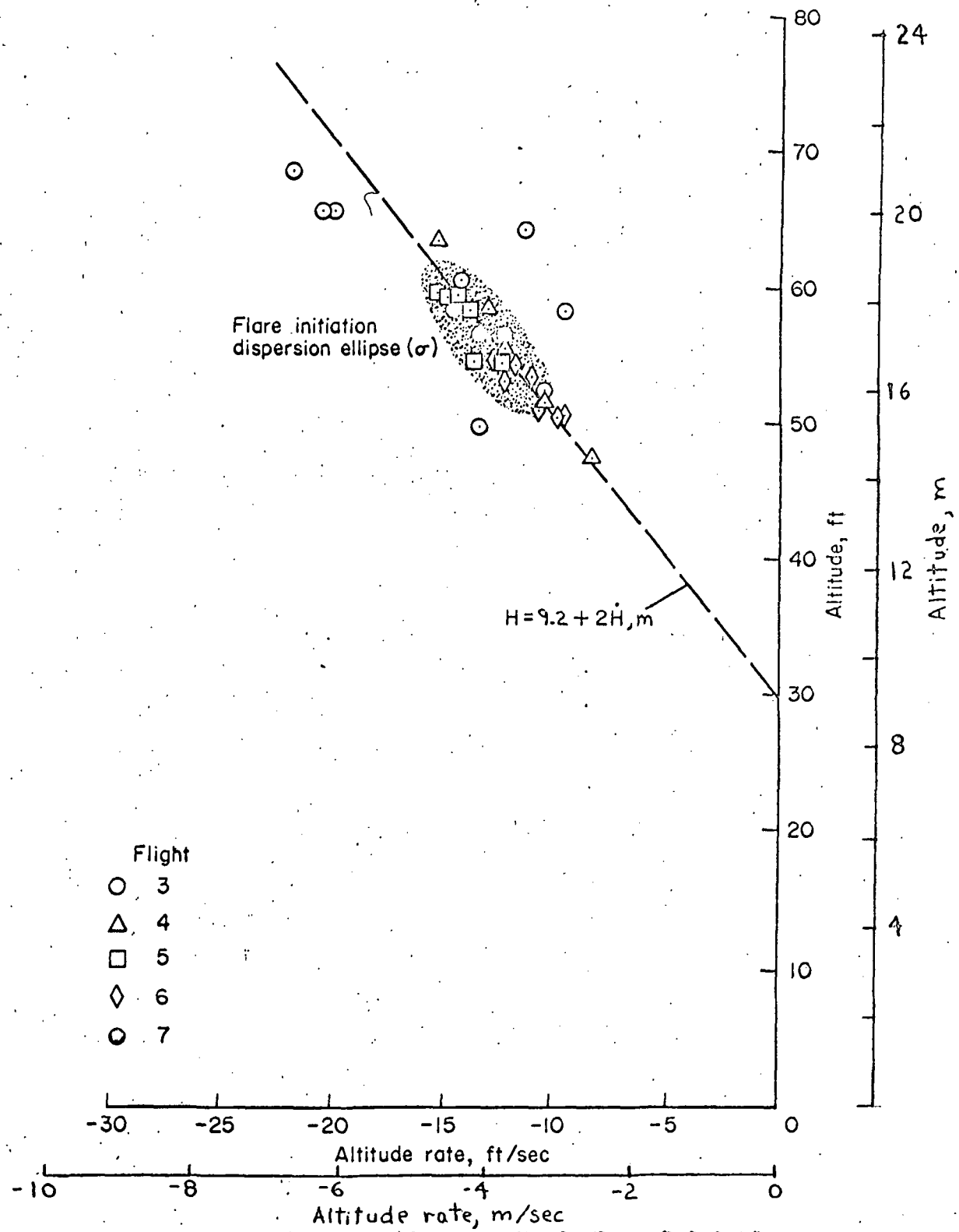

Figure 15. - Dispersions at Final Flare Initiation

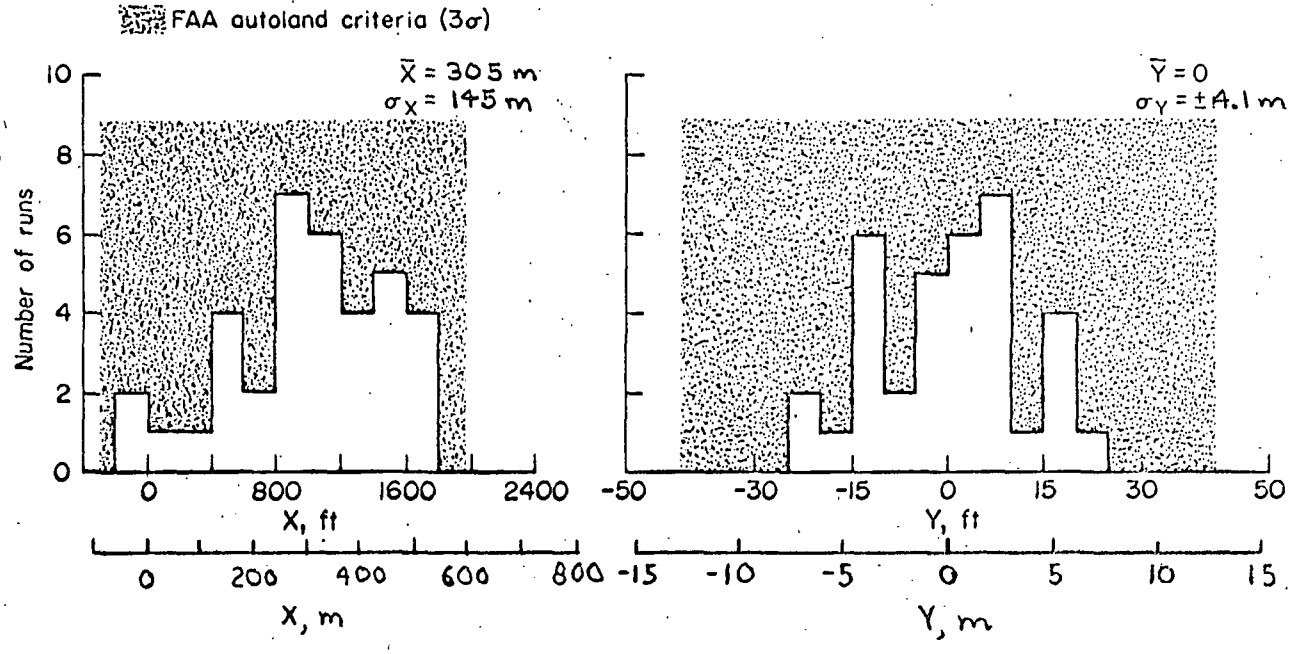

(a) Longitudinal Dispersions

(b) Lateral Dispersions

Figure 16. - Position Dispersions at Touchdown

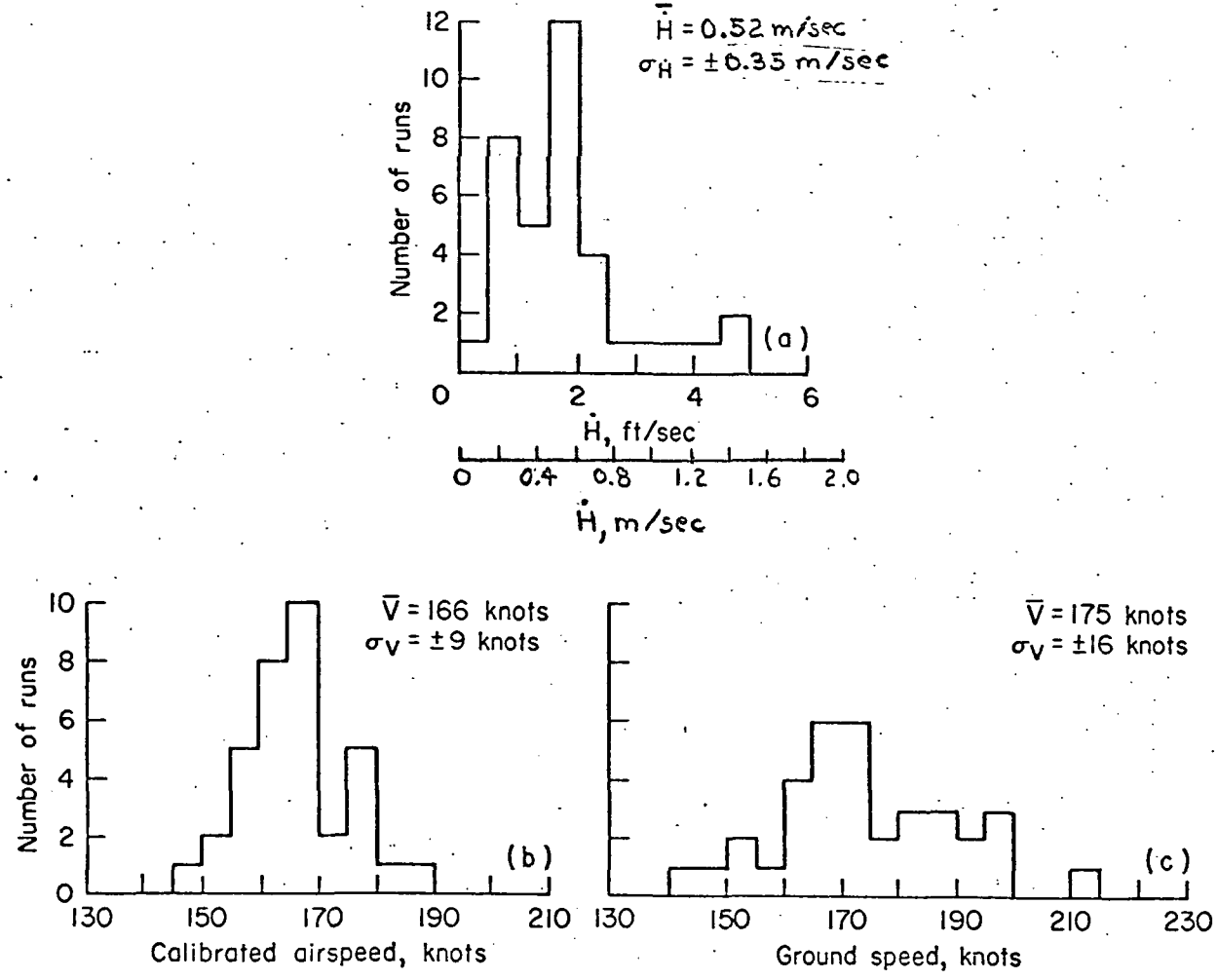

(a) Vertical Speed
(b) Calibrated Airspeed
(c) Ground Speed

Figure 17. - Speed Dispersions at Touchdown

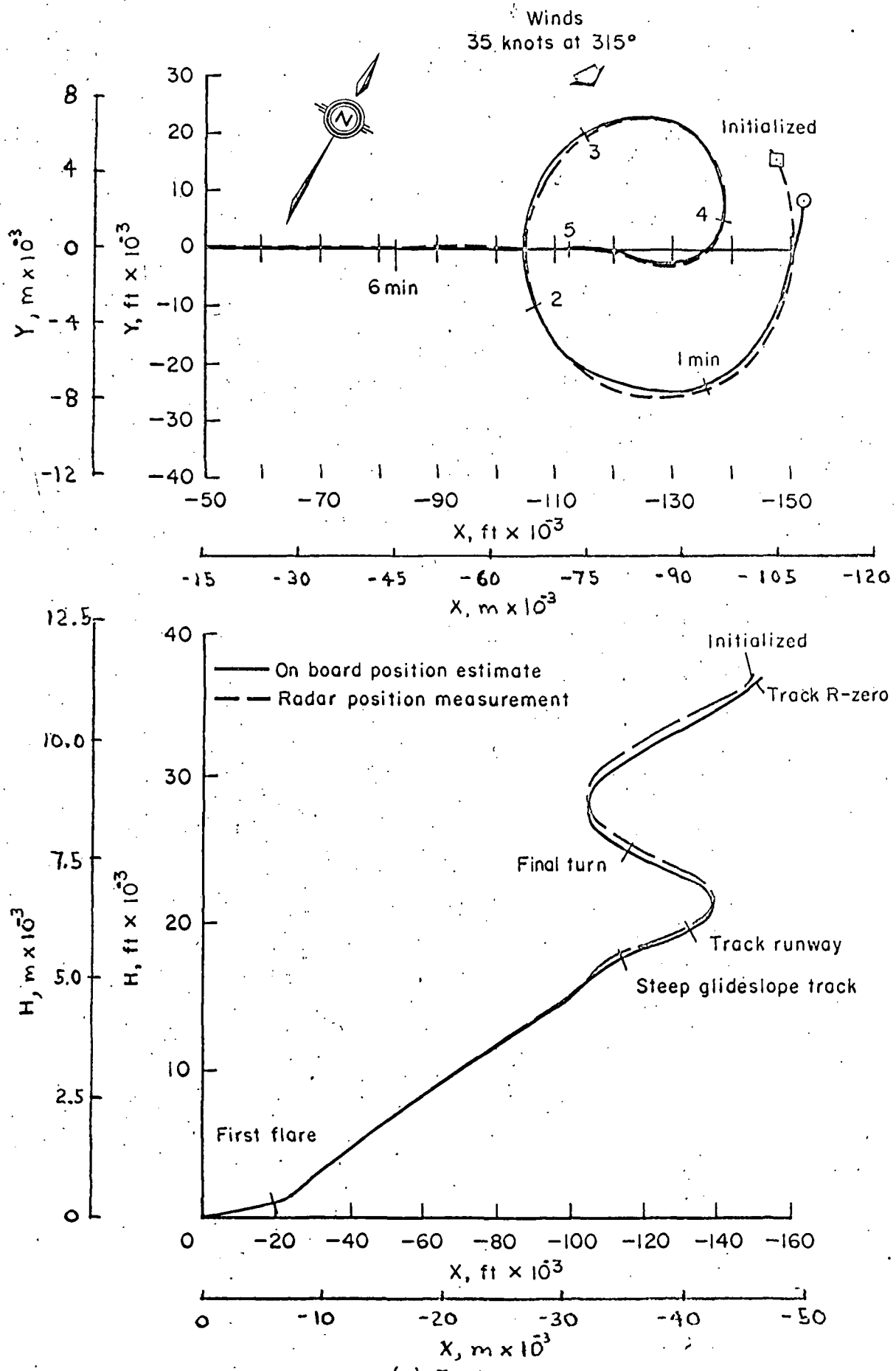

(a) Trajectory Plot.

Figure 18. - Navigation Performance During Approach

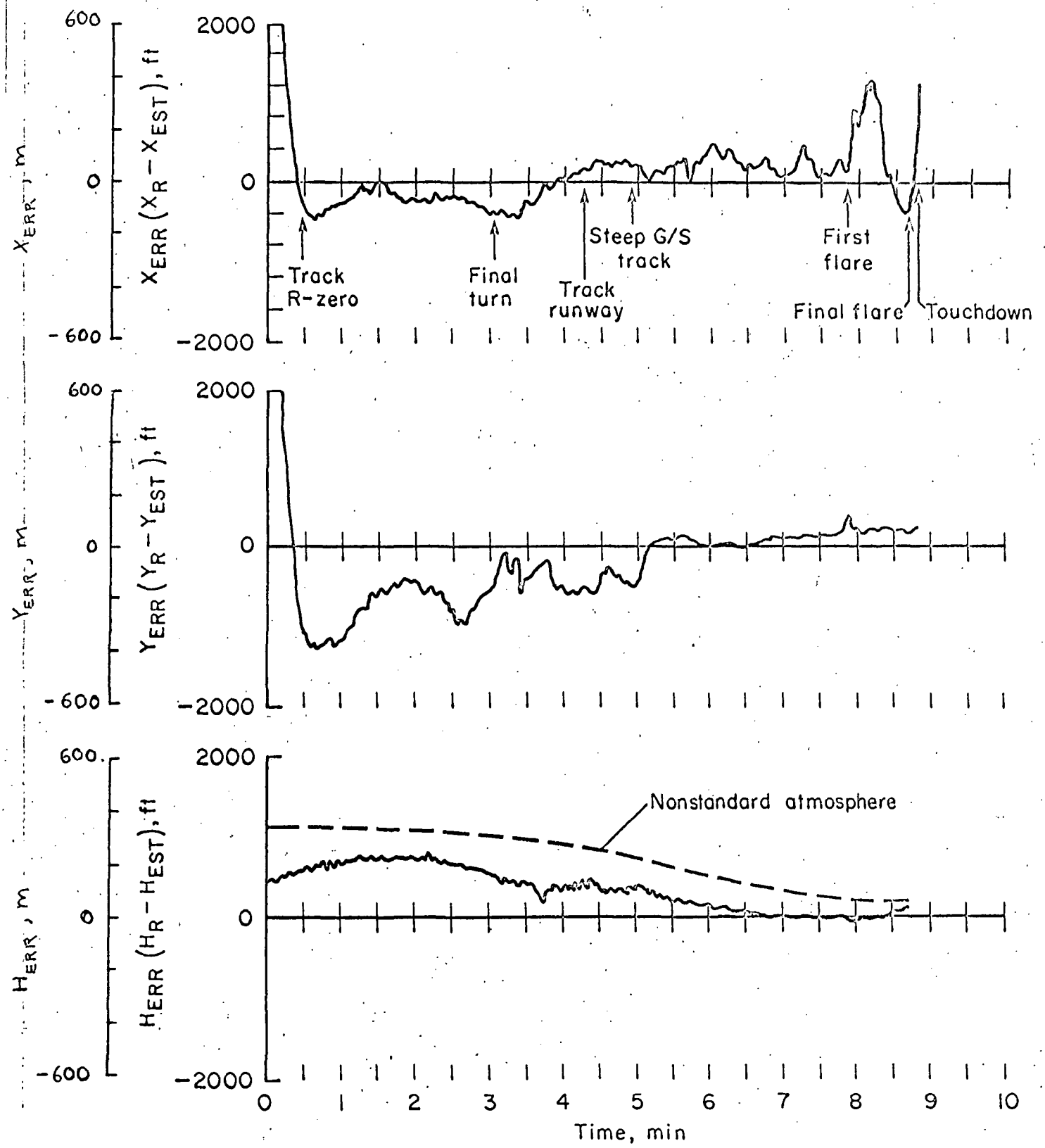

(b) Time Histories of Navigation Errors

Figure 18. - Concluded

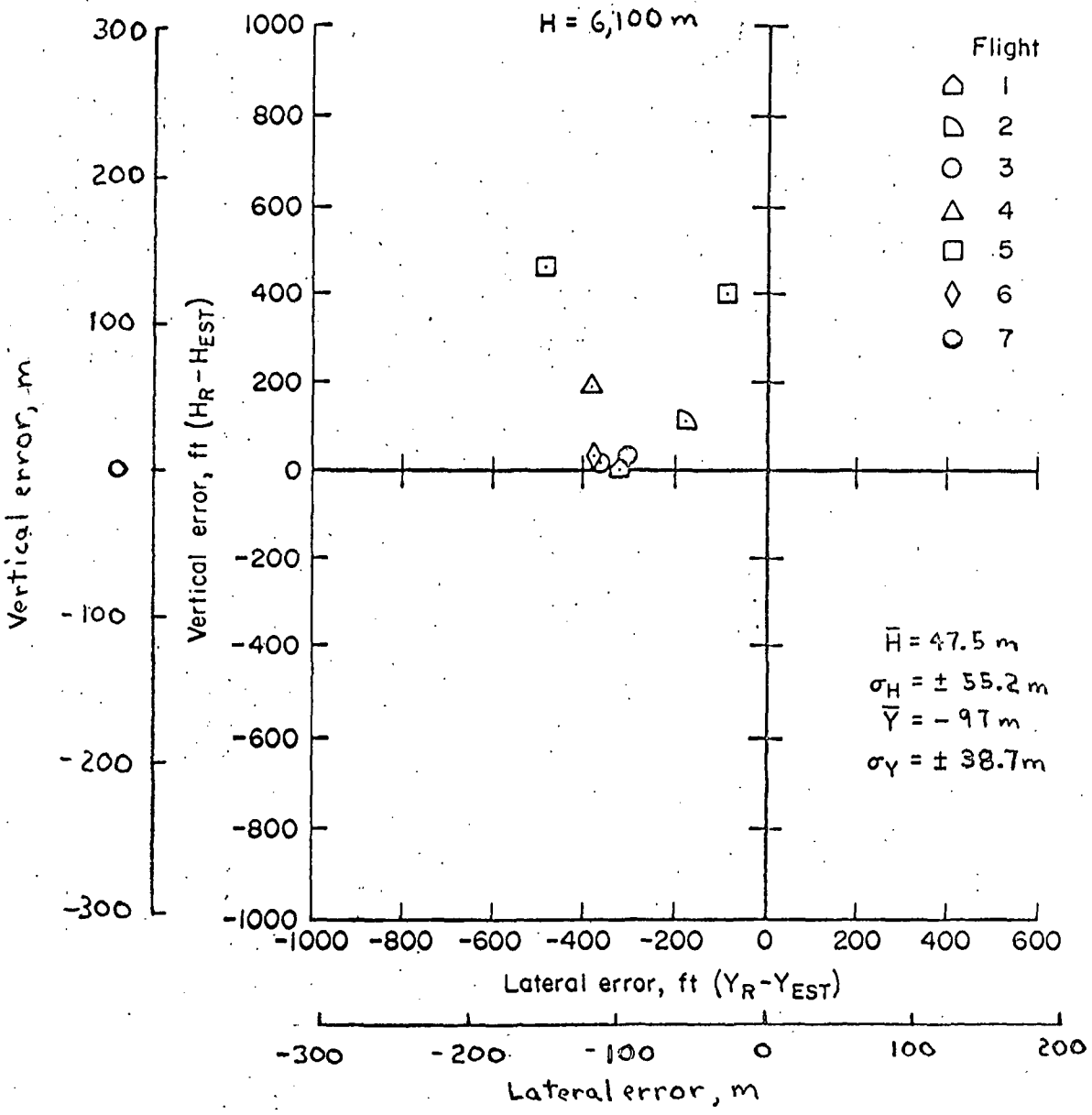

Figure 19. - Navigation Errors at Steep Glide Slope Capture Window

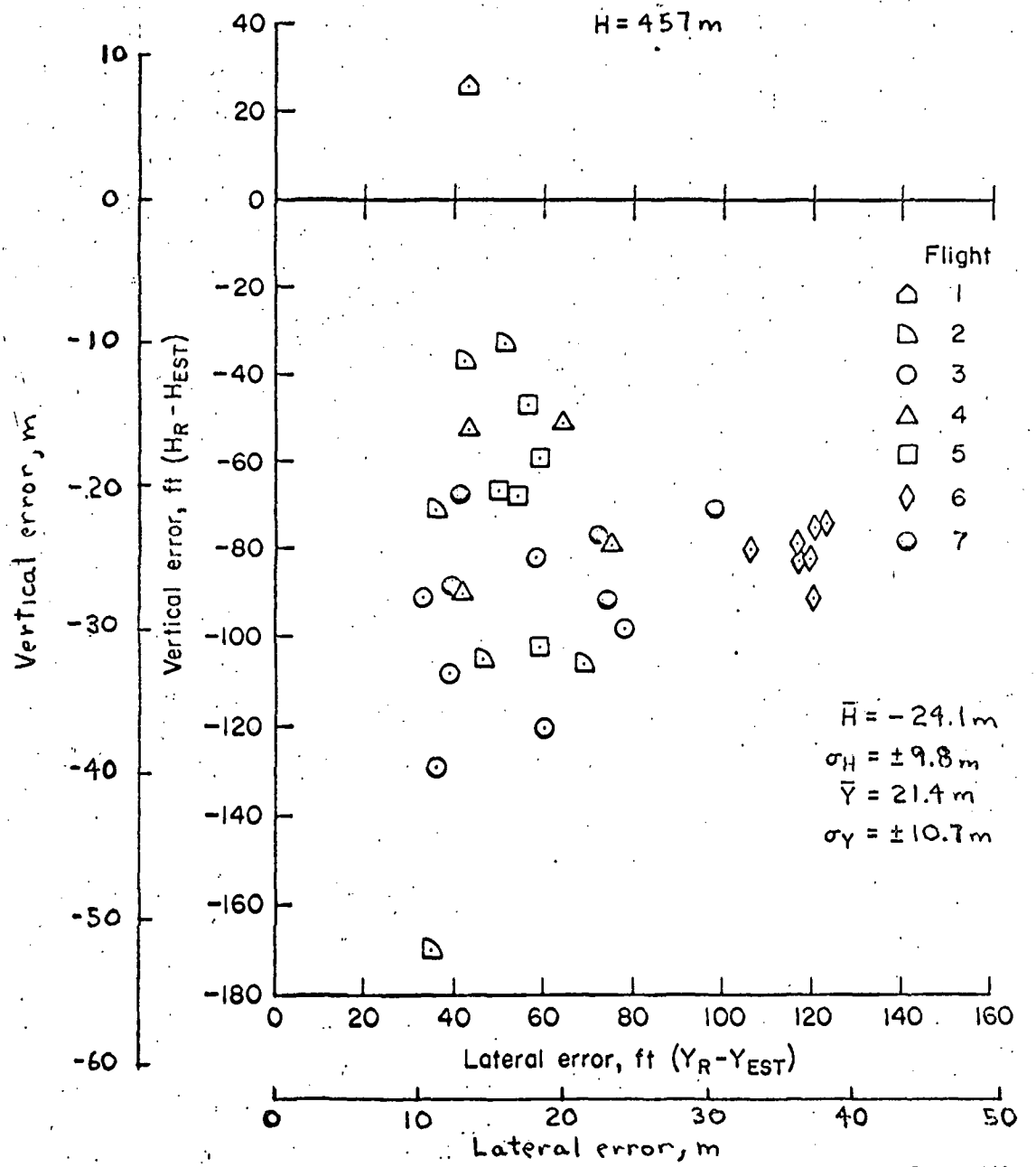

Figure 20. - Navigation Errors at First Flare Window

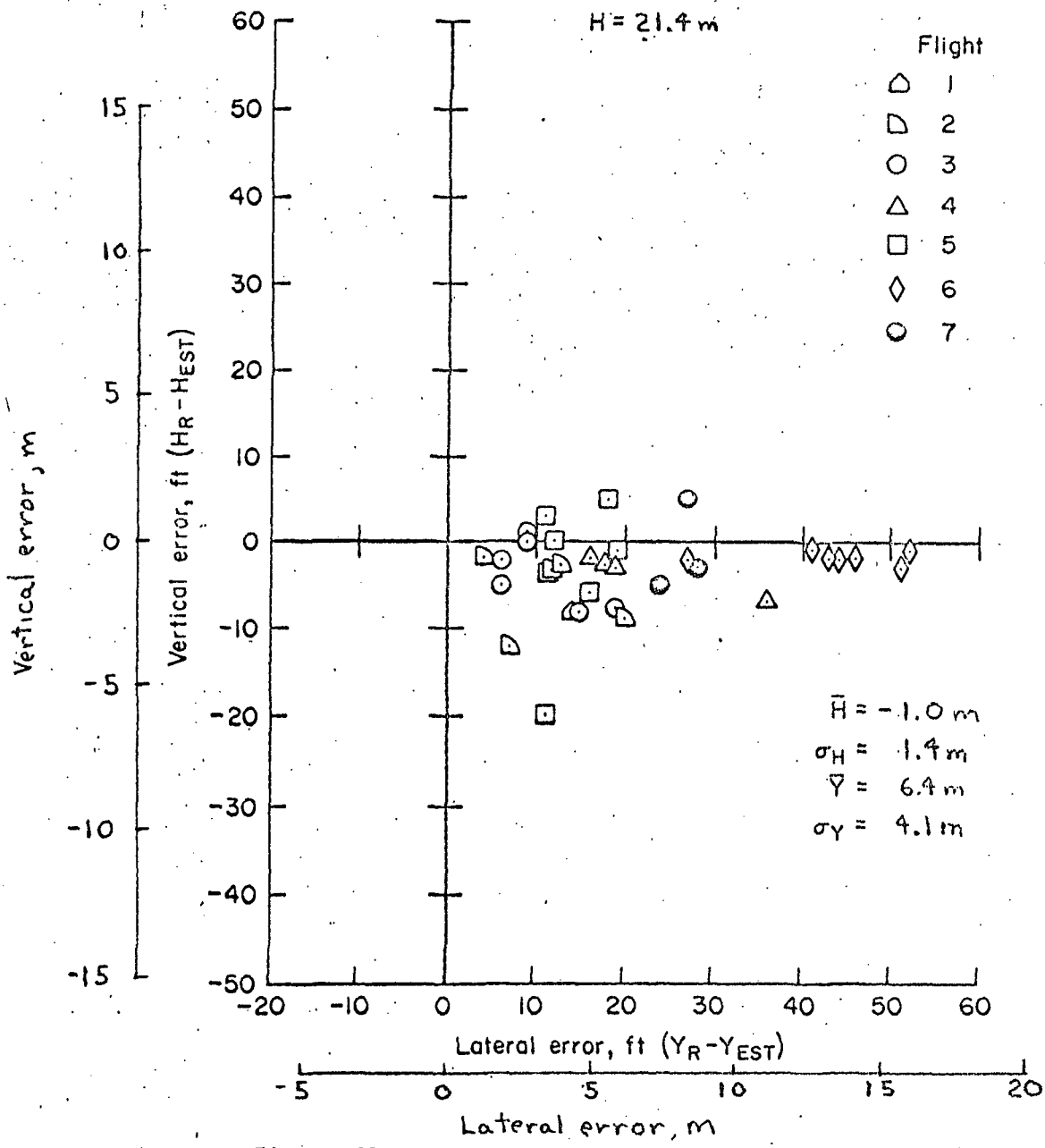

Figure 21. - Navigation Errors at Final Flare Window